

**METHODS TO INDUCE A PREFERRED MOLECULAR ALIGNMENT IN THE  
EPITAXIAL GROWTH OF *n*-ALKANE THIN FILMS**

A Thesis Submitted to the College of  
Graduate Studies and Research  
in Partial Fulfillment of the Requirements  
for the Degree of Master of Science  
in the Department of Chemistry  
University of Saskatchewan  
Saskatoon, SK.

By  
AMARA ZUHAIB

## **PERMISSION TO USE**

In presenting this thesis in partial fulfillment of the requirements for a postgraduate degree from the University of Saskatchewan, I agree that the libraries of this University may make it freely available for inspection. I further agree that permission for copying of this thesis in any manner, in whole or in part for scholarly purposes may be granted by Professor Stephen G. Urquhart who supervised my thesis work or in his absence by the Head of the Department of Chemistry or the Dean of the College of Graduate Studies and Research. It is understood that any copying, publication, or use of this thesis or parts thereof for financial gain shall not be allowed without my written permission. It is also understood that due recognition shall be given to me and to the University of Saskatchewan in any scholarly use that may be made of any material in my thesis. Request for permission to copy or to make other use of material in this thesis in completely or in part should be addressed to:

The Head

Department of Chemistry

University of Saskatchewan

Saskatoon, Saskatchewan

Canada S7N 5C9

## ABSTRACT

The development of general techniques to define and control the molecular orientation at the nanoscale can improve the efficiency of some functional materials, such as organic electronic devices, waveguides and liquid crystal based devices. The main aim of this project is to develop methods to define and control the orientation and ordering of molecules in the epitaxially grown organic thin films. There are a number of factors such as field effects (magnetic and electric), temperature, and substrate crystal lattice orientation, which can be tailored to achieve the molecular orientation control.

The first method to control the molecular orientation control was based upon the concept of liquid crystal imprinting (LCI) technique developed by the Patrick group (Western Washington University, USA) in which an oriented monolayer *n*-alkane film was grown by epitaxy on a liquid crystal (LC) film on a graphite substrate, where the LC film was initially oriented by using a magnetic field. The first goal of this research work was to reproduce this LCI work for oriented *n*-alkane multilayer films. A LC film can act as a sacrificial template and the magnetic field can initially align LC thin films on the graphite substrate. Then, *n*-alkanes deposited by physical vapour deposition can diffuse through the LC and replace the oriented LC molecules while preserving their orientation, leading to oriented *n*-alkane films.

The second goal of research project is to develop a new method for controlling the molecular orientation of *n*-alkane films. The idea of LCI was modified and in the new method LC films are oriented with an electric field. Then, thin films of *n*-tetracontane (C<sub>40</sub>, C<sub>40</sub>H<sub>82</sub>) are subsequently deposited on the electrically oriented LC by physical vapour deposition. In this process, the oriented LC film acts as a sacrificial template and highly oriented *n*-alkane films are obtained.

In this research work, the results of Patrick *et al.*<sup>1</sup> were reproduced and the idea of LCI was extended to electric field alignment for obtaining highly oriented *n*-alkane films.

## ACKNOWLEDGEMENTS

During the two years of my studies, many people have given me their guidance and help. I would like thus at the end of this thesis to express my thanks to all of them. First, I would like to address my sincere gratitude to Prof. Dr. Stephen G. Urquhart. His supervision was the foundation for all my gains. His integral views, unique insights, abundant experiences and immense knowledge inspired and enriched me as a student and researcher. Besides his supervision and help in my study, his passions, patience and enthusiasm have influenced and enhanced my own character. It is a pleasure to have the chance of working with him.

My advisory committee: Dr. Andrew Grosvenor and Dr. Stephen G. Urquhart deserve credit for their advice and constructive criticism throughout my project.

I wish to thank the University of Saskatchewan, the Department of Chemistry and its staff, electronic shop of chemistry department and physics machine shop. I am thankful to Dr. R. Sammynaiken for allowing me to use the EPR magnets from the SSSC labs. In addition, I want to thanks Micheal Sigrist from CLS for giving me the permission to use dipole magnets from the magnet mapping lab.

I would like to thank all colleagues and friends who worked together with me during these years, especially Sahan Perera and Mitra Masnadi.

I thank all my family members my parents and parents-in-law, sisters and brothers who have been constantly loving and supporting me. They give me strength when I am weak; they give me persuasions when I am frivolous; they give me encouragements when I am frustrated and they give me applauds when I am progressing.

I am extremely grateful to my husband Zuhaib, who always encourage me in every step of my life. I am so happy to have you in my life, and I love you so much. Finally, my kids, my life

Eshal and Abdul Haady, I could have never achieved my goals without their love and support all the time.

## TABLE OF CONTENTS

<b>PERMISSION TO USE .....</b>	<b>i</b>
<b>ABSTRACT.....</b>	<b>ii</b>
<b>ACKNOWLEDGEMENTS .....</b>	<b>iv</b>
<b>TABLE OF CONTENTS .....</b>	<b>vi</b>
<b>LIST OF FIGURES .....</b>	<b>ix</b>
<b>LIST OF TABLES .....</b>	<b>xv</b>
<b>LIST OF ABBREVIATIONS .....</b>	<b>xvi</b>
<b>Chapter 1: INTRODUCTION.....</b>	<b>1</b>
1.1 Epitaxy.....	1
1.1.1 Epitaxial Growth of Hydrocarbon Thin Films .....	2
1.1.2 Techniques for the Preparation of Epitaxial Thin Films .....	5
1.1.3 Molecular Orientation and the Mechanism of Epitaxial Growth.....	6
1.2 Orientation Control in Thin Films and its Importance .....	9
1.2.1 Orientation Control Using LC Imprinting .....	11
1.2.2 Effect of Magnetic Field on LC Orientation .....	16
1.2.3 Effect of Electric Field on LC Orientation.....	16
1.3 Research Approaches .....	18
<b>Chapter 2: EXPERIMENTAL APPARATUS .....</b>	<b>19</b>
2.1 Heating Cell.....	19
2.2 High Field Dipole Magnets for Sample Alignment .....	20
2.3 Evaporator for Physical Vapour Deposition.....	23
2.4 Electric Field Alignment .....	25
2.5 Electrode Formation .....	25

2.6 Optical Microscopy .....	26
<b>Chapter 3: EXPERIMENTAL WORK .....</b>	<b>30</b>
3.1 Orientation Control by Magnetically Oriented LCI .....	30
3.1.1 Experimental Approach .....	30
3.1.2 Sample Preparation .....	30
3.1.2.1 <i>N</i> -Alkane and LC Candidates .....	30
3.1.2.2 Substrate Selection.....	33
3.1.2.3 LC Film Preparation and its Alignment.....	34
3.1.2.4 C40 Deposition by Solution Casting .....	35
3.1.2.5 Preparation of C40 Thin Films by PVD .....	36
3.1.3 Characterization of <i>n</i> -Alkane Films .....	36
3.2 Orientation Control by Electric Field Alignment .....	37
3.2.1 Experimental Approach .....	37
3.2.2 Sample Preparation for Electric Field Alignment .....	37
3.2.2.1 Substrate Selection.....	37
3.2.2.2 LC Film Preparation .....	37
3.2.2.3 Application of Electric Field .....	38
3.2.2.4 C40 Deposition .....	38
3.2.3 Characterization of Thin Films .....	38
<b>Chapter 4: RESULTS AND DISCUSSION.....</b>	<b>39</b>
4.1 LC Film Preparation on HOPG .....	39
4.2 Effect of Magnetic Field Strength on the Orientation of <i>n</i> -Alkane Films.....	47
4.2.1 Effect of Magnetic Field between 0.2 T - 2.0 T .....	48
4.2.2 Effect of Magnetic Field between 2.0 T - 2.3 T .....	50



4.3 Discussion.....	53
4.4 <i>N</i> -Alkane Film Preparation on Electrically Aligned LC .....	56
4.4.1 <i>N</i> -Alkane Film Preparation on Different Samples .....	56
4.5 Discussion.....	60
4.6 Experimental Challenges .....	62
<b>Chapter 5: CONCLUSIONS.....</b>	<b>64</b>
<b>Chapter 6: FUTURE WORK .....</b>	<b>66</b>
<b>REFERENCES.....</b>	<b>67</b>

## LIST OF FIGURES

### CHAPTER 1

- Figure 1.1:** Different growth modes observed during epitaxial growth (a) layer-by-layer, Frank-van der Merwe growth (2D model), (b) layer-plus-island, Stranski-Krastonov growth (2D and 3D model), (c) island structures, Volmer-Weber growth (3D model). This figure is derived from reference 2..... 5
- Figure 1.2:** Orientation of linear organic molecules on a substrate (a) In plane or parallel orientation of *n*-alkane molecules. (b) Normal or vertical orientation of *n*-alkane molecules. The long axis of the *n*-alkane is represented by a straight line. .... 6
- Figure 1.3:** Plot of lateral orientation fraction of C<sub>40</sub>H<sub>82</sub> thin film against the substrate temperature (°C). This figure is reprinted from reference 26 with permission. .... 7
- Figure 1.4:** Thin film formation on a substrate. (1) adsorption from vapour, (2) migration, (3) re-evaporation from substrate, (4) cluster formation, (5) re-evaporation from cluster, (6) reorientation. This figure is reprinted from reference 29 with permission. .... 9
- Figure 1.5:** Schematic of the experimental set up for electrical field induced patterning in diblock copolymer films. This figure is reprinted from reference 38 with permission. .... 10
- Figure 1.6:** Structure of LC, 8CB (4-octyl-4-cyanobiphenyl) molecule..... 12
- Figure 1.7:** (a) Nematic phase of LC (b) Smectic phase of LC, the vector *n* represents the director of the LC molecules. This figure is reprinted from reference 46 with permission. .... 13
- Figure 1.8:** Liquid Crystal Imprinting (LCI) in which LC molecules are aligned parallel to the applied magnetic field and these LCs act as a template layer for aligning subsequently deposited organic molecules. This figure is reprinted from reference 48 with permission. .... 14

<b>Figure 1.9:</b> Proposed model by Patrick's group in which LC (8CB) molecules are replaced by C40 molecule. Initially 8CB is oriented parallel to the magnetic field. This image is reprinted from reference 1 with permission. ....	15
<b>Figure 1.10:</b> Effect of electric field on the orientation of LC molecules. This figure is derived from reference 45. The blue arrows represent the electric field vector (E) while the black arrows show the electric force (F) on the molecule. ....	17
<b>Figure 1.11:</b> Behaviour of molecules with positive dielectric constant value in an electric field. ....	17
<b>CHAPTER 2</b>	
<b>Figure 2.1:</b> (a) Heating cell with heater and ceramic thermal plates isolation. (b) Two different sizes of heating cells. ....	20
<b>Figure 2.2:</b> Bruker EMX-EPR Spectrometer in the Saskatchewan Structural Science Centre (SSSC).....	21
<b>Figure 2.3:</b> Experimental setup for magnetic field alignment using Danfysik system 8000, magnetic system in magnet mapping lab (CLS). ....	22
<b>Figure 2.4:</b> Teslameter for measuring magnetic strength from magnet mapping lab (CLS). ....	22
<b>Figure 2.5:</b> Plot of the relationship between pole face gaps (mm) and magnetic field (T). <sup>53</sup> .....	23
<b>Figure 2.6:</b> Vacuum evaporator. ....	24
<b>Figure 2.7:</b> (a) Vacuum chamber external view. (b) Vacuum chamber internal view.	24
<b>Figure 2.8:</b> Sample holder with copper plate on top of Peltier heater. ....	25
<b>Figure 2.9:</b> (a) 70 nm thick gold layer deposited on Si <sub>3</sub> N <sub>4</sub> window at room temperature by PVD. (b) Schematic diagram of the LC orientation experiment. ....	26

**Figure 2.10:** (a) 70 nm thick gold layer deposited on Si<sub>3</sub>N<sub>4</sub> window at room temperature by PVD. (b) Schematic diagram of the LC orientation experiment. .... 27

**Figure 2.11:** Schematic illustration of bright and dark field epi-illumination. This figure is reprinted from reference 55. .... 27

**Figure 2.12:** The effect of birefringent sample and polarizers in the transmission of light. This figure is reprinted from reference 57. .... 29

### CHAPTER 3

**Figure 3.1:** DSC spectrum of *n*-tetracontane. .... 31

**Figure 3.2:** DSC spectrum of 8CB (4-octyl-4-cyanobiphenyl). .... 32

**Figure 3.3:** Polarized optical microscope images of the samples having (a) freshly peeled Kish graphite on a clean Si(111) surface. (b) freshly cleaved HOPG surface, at 50X objective lens magnification and bright field illumination. .... 33

**Figure 3.4:** Position of sample within the dipole magnets in magnetic mapping lab (CLS) during the alignment experiment. .... 35

**Figure 3.5:** Process of thin film formation during the physical vapour deposition (PVD). .... 36

### CHAPTER 4

**Figure 4.1:** Polarized optical microscope images of the samples prepared by depositing (a) LC gel on Kish graphite on the silicon wafer sample at room temperature. (b) LC on Kish graphite on the silicon wafer after heating and spreading the LC gel with a glass coverslip. (c) LC on HOPG after heating and distributing by glass coverslip at 100X objective lens magnification and bright field illumination. .... 39

<b>Figure 4.2:</b> Polarized optical microscope image of a sample prepared by depositing C40 on oriented LC on HOPG by solution deposition method at 100X objective lens magnification and bright field illumination. ....	40
<b>Figure 4.3:</b> Polarized optical microscope image of a sample prepared by depositing C40 on LC on HOPG-ZYH substrate by PVD at 36 °C substrate temperature, at 100X objective lens magnification and bright field illumination. ....	41
<b>Figure 4.4:</b> Polarized optical microscope images of the samples prepared by depositing C40 on (a) Kish graphite at 25 °C substrate temperature, (b) freshly cleaved HOPG at 36 °C substrate temperature and (c) freshly cleaved HOPG at 42 °C substrate temperature, at 100X objective lens magnification and bright field illumination. ....	43
<b>Figure 4.5:</b> Polarized optical microscope images of the samples prepared by depositing C40 (a) in the absence of LC at 50 °C (b) in the presence of pure LC at 50 °C, at 100X objective lens magnification and bright field illumination. ....	44
<b>Figure 4.6:</b> Polarized optical microscope images of the sample prepared by depositing LC on (a) HOPG-ZYH substrate (b) Kish graphite on the Si wafer substrate at room temperature, at 100X objective lens magnification and bright field illumination. ....	46
<b>Figure 4.7:</b> Polarized optical microscope image of a sample prepared by depositing C40 thin film on diluted LC with no magnetic field alignment, on HOPG, at 36 °C substrate temperature, at 100X objective lens magnification and bright field illumination. ....	46
<b>Figure 4.8:</b> Polarized optical microscope image of a sample prepared by diluted 8CB thin film on HOPG substrate (a) before and (b) after alignment in a magnetic field at 100X objective lens magnification and bright field illumination. ....	47

<b>Figure 4.9:</b> Polarized optical microscope images (magnified) of the samples prepared by depositing C40 on HOPG substrate at 36 °C, on top of diluted LC in the presence of different magnetic field strengths of (a) 0.2 T, (b) 0.7 T and (c) 1.0 T respectively at 100X objective lens and bright field illumination. The arrow sign is indicating the direction of magnetic field. ....	48
<b>Figure 4.10:</b> Polarized optical microscope images of C40 deposition on Kish graphite on the Si wafer substrate on top of diluted LC in the presence of different magnetic field strengths of (a) 0.2 T, (b) 0.7 T at 100X and (c) 1.0 T at 50X objective lens magnifications and bright field illumination. ....	49
<b>Figure 4.11:</b> Polarized optical microscope images of the samples prepared by depositing C40 by PVD on HOPG at 36 °C substrate temperature on magnetically aligned diluted LC at different magnetic field strengths of (a) 1.2 T, (b) 1.5 T and (c) 2.0 T at 100X objective lens magnification and bright field illumination. ....	50
<b>Figure 4.12:</b> Polarized optical microscope images of the samples prepared by depositing C40 thin film on dilute LC on HOPG at 36 °C substrate temperature, after applying a magnetic field of (a) 2.1 T, (b) 2.2 T (c) 2.3 T and (d) magnified image after applying a magnetic field of 2.3 T at 100X objective lens magnification (e) 2.3 T at 50X objective lens magnification and bright field illumination.....	51
<b>Figure 4.13:</b> Step-by-step process of the LCI method for obtaining oriented C40 film using the LCI method. <sup>1</sup> .....	52
<b>Figure 4.14:</b> Polarized optical microscopic image (magnified) of a sample prepared by depositing C40 having vertically oriented <i>n</i> -alkane bars on HOPG substrate at 36 °C substrate temperature at 100X objective lens magnification and bright field illumination. ....	54

<b>Figure 4.15:</b> Parallel (side-by-side) position of C40 molecules in a bar like structures, on the basis of the model proposed by J. Fu <i>et al.</i> <sup>23</sup> .....	54
<b>Figure 4.16:</b> Polarized optical microscope image a sample having a LC thin film on freshly cleaved NaCl substrate at 100X objective lens magnification and dark field illumination.....	57
<b>Figure 4.17:</b> Polarized optical microscope images of the samples prepared by depositing C40 on (a) NaCl(001) substrate at 36 °C substrate temperature (b) NaCl(001) substrate having diluted LC at 36 °C substrate temperature without applying electric field, at 100X objective lens magnification and bright field illumination. ....	58
<b>Figure 4.18:</b> Polarized optical microscope image (magnified) of a sample prepared by depositing C40 thin films on NaCl substrate having bars at 90° to each other at 100X objective lens magnification and bright field illumination. ....	58
<b>Figure 4.19:</b> Polarized optical microscope images of a sample prepared by depositing <i>n</i> -alkane film on electrically oriented LC on NaCl(001) substrate at 36 °C substrate temperature, having (a) 4-fold symmetry (b) broken 4-fold symmetry (c) vertically oriented <i>n</i> -alkane bars at 100X objective lens magnification and bright field illumination. ....	59
<b>Figure 4.20:</b> Polarized optical microscope images of a sample prepared by depositing C40 film on NaCl (001), with electrically oriented LC, on NaCl(001) substrate at 36 °C substrate temperature having (a) all three different morphologies of C40 orientation (b) vertically oriented <i>n</i> -alkane bars (c) 4-fold symmetry (d) broken 4-fold symmetry at 100X objective lens magnification and bright field illumination. ....	60

## LIST OF TABLES

<b>Table 1:</b> Comparison of phase transition values among literature and DSC values .....	32
---	----



## LIST OF ABBREVIATIONS

AFM	Atomic Force Microscopy
CLS	Canadian Light Source
C32	<i>n</i> -dotriacontane (C <sub>32</sub> H <sub>66</sub> )
C40	<i>n</i> - tetracontane (C <sub>40</sub> H <sub>82</sub> )
8CB	4-Octyl-4-Cyanobiphenyl
DSC	Differential Scanning Calometry
EPR	Electron Paramagnetic Resonance (magnets)
FM	Frank-van der Merwe
HOPG	Highly Oriented Pyrolytic Graphite
IRRAS	Infrared Reflection Absorption Spectroscopy
LEED	Low Energy Electron Diffraction
LC	Liquid Crystal
LCD	Liquid Crystal Display
LCI	Liquid Crystal Imprinting
PVD	Physical Vapour Deposition
Si	Silicon
SK	Stranski-Krastonov
STM	Scanning Tunneling Microscopy
SEM	Scanning Electron Microscopy
SSSC	Saskatchewan Structural Science Centre
VW	Volmer-Weber

## CHAPTER 1

### INTRODUCTION

Orientation control is crucial for the development of electro-optical thin film devices, as the physical properties of these devices depend upon molecular orientation. The main focus of this project is to develop methods to control the orientation and ordering of molecules in organic thin films at the nanoscale, based upon the concept of liquid crystal imprinting (LCI)<sup>1</sup> for epitaxially grown *n*-alkane thin films. In Chapter 1, section 1.1, modes of organic film growth and molecular orientation during thin film growth are discussed in detail. In section 1.2, the importance of orientation control in thin films is discussed along with the review of previous methods for controlling molecular orientation in thin films. Research methods used to attain the research objectives are discussed in section 1.3. In Chapter 2, the experimental apparatus are discussed in detail, while Chapter 3 deals with sample preparation. Chapter 4 presents the results along with the discussion of these results.

#### 1.1 Epitaxy

This term epitaxy was defined in 1928 and refers to the oriented growth of one substance on the surface of another substance.<sup>2</sup> Epitaxy comes from the Greek origin *epi* (επι-), meaning "above", and *taxis* (ταξι-), meaning "in ordered manner".<sup>3</sup>

In general, epitaxy is applied to molecular films grown on some crystalline substrate in such a manner that the guest molecular chains copy the host crystal lattice orientation with their chain axis parallel to the substrate surface. Molecules in the subsequently deposited layers follow the molecular orientation in the preceding layers, making oriented multilayer films.<sup>4</sup>

According to Forrest,<sup>5</sup> epitaxy in inorganic materials occurs when there is a commensurate relationship between the depositing material and the substrate. In case of organic epitaxy, this

commensurate (one-to-one) relationship is not a basic requirement. Epitaxy is a broad term including both the atomic and molecular epitaxy. An example for atomic epitaxy includes the deposition of silicon on a silicon substrate.<sup>6</sup>

In the case of atomic epitaxy, crystal strain and lattice matching are the critical factors, while in case of molecular epitaxy, molecular orientation and molecular flexibility are the key factors. Orientation is absent in case of atomic epitaxy.<sup>7</sup> An example of molecular epitaxy is the deposition of *n*-alkane thin films on the surface of highly oriented pyrolytic graphite (HOPG).<sup>7</sup> The definition of epitaxy can be divided into homoepitaxy and heteroepitaxy. Homoepitaxy is the growth of the same material onto itself. The film-substrate interface diminishes into the bulk material, so that the interfacial energy  $\gamma_i$  becomes zero. In case of heteroepitaxy, which is the growth of one material on top of a different material, the interfacial energy is  $\gamma_i > 0$ , and the molecules will align in the direction giving a smaller  $\gamma_i$  with maximum surface bonding.<sup>8</sup> When there is a chemical bond between the adsorbed layer and substrate then this epitaxy is known as conventional epitaxy.<sup>9</sup> On the contrary, when there is a physical interaction between the adsorbate and adsorbent, then this epitaxy is called van der Waals epitaxy.<sup>10</sup>

In 1950, Kainuma and Uyeda<sup>11</sup> observed the ordered organic molecules on a single crystalline substrate. Suito *et al.*<sup>12</sup> introduced the terminology “epitaxial growth” for organic molecules, based on deposition of a thin layer of phthalocyanine on mica.

### 1.1.1 Epitaxial Growth of Hydrocarbon Thin Films

Epitaxial growth can be used to prepare well-ordered hydrocarbon thin films. Alkali halides (NaCl, KCl etc) are common substrates for the epitaxial growth of the organic materials.<sup>13,14</sup> Mauritz *et al.*<sup>15,16</sup> studied the growth of polyethylene on NaCl substrate. They suggested that for the minimum energy orientation, polymers chains should be parallel to the substrate with the

alignment of the polymer chains along the  $\langle 110 \rangle$  and  $\langle \bar{1}10 \rangle$  surface directions, along orthogonal arranged rows of  $\text{Na}^+$  ions. The high symmetry of the  $\text{NaCl}(001)$  surface and the low crystal lattice orientation enables the parallel orientation of  $n$ -alkane chains along the  $\langle 110 \rangle$  and  $\langle \bar{1}10 \rangle$  direction.

Hentschke *et al.*<sup>17</sup> examined  $n$ -alkane molecules ( $\text{C}_{13}\text{H}_{28}$ ) capable of forming well-ordered layers on graphite. Similar results were obtained with  $\text{C}_{50}\text{H}_{102}$  at room temperature, while the shorter alkane ( $< \text{C}_{13}$ ) cannot develop these kinds of structures due to their surface mobility. Hosoi *et al.*<sup>18</sup> studied the long chain  $n$ -alkane  $\text{C}_{44}\text{H}_{90}$  thin films on a  $\text{Cu}(100)$  single crystal surface by infrared reflection absorption spectroscopy (IRRAS) and low energy electron diffraction (LEED). IRRAS revealed that the first layer is different from the bulk during the epitaxial film growth on  $\text{Cu}(100)$  and LEED reflects intramolecular periodicity.

*In situ* scanning tunneling microscopy (STM) study by Rabe *et al.*<sup>19</sup> revealed that  $n$ -alkane and other organic molecules can be deposited on graphite substrates and showed that these alkane molecules can organize themselves as lamellae, having long chain axis parallel to the substrate basal plane.

Leunissen and coworkers<sup>20</sup> developed a solution deposition process model for the  $n$ -alkane epitaxial film growth and their results showed in-plane orientation on a graphite substrate for  $\text{C}_{32}\text{H}_{66}$  and  $\text{C}_{33}\text{H}_{68}$ . They proposed a Stranski-Krastanov growth model (discussed below) for the three dimensional growth of  $n$ -alkane films on top of a monolayer attached to the graphite. They used scanning electron microscopy (SEM), polarized optical microscopy and atomic force microscopy (AFM) to characterize their results.

Cincotti *et al.*<sup>21</sup> studied the interaction of the  $n$ -alkane molecule dotriacontane ( $\text{C}_{32}\text{H}_{66}$ ) on  $\text{MoS}_2$  and  $\text{MoSe}_2$  substrates. They revealed that during the physisorption, surface flatness plays a vital

role in the formation of highly ordered structures while the role of the surface lattice plays a minor role. Shimizu *et al.*<sup>22</sup> studied the temperature effect on the molecular orientation for *n*-alkane molecules ( $C_{40}H_{82}$  -  $C_{60}H_{122}$ ) and reported normal orientation (perpendicular to the substrate) in films that are deposited at higher temperature. This signifies that molecular orientation is not only governed by the interaction between deposit and substrate, but that growth kinetics also plays a pivotal role in determining molecular orientation.

During the epitaxial growth of organic molecules, two different molecular orientations have been observed. The work of Fu *et al.*<sup>23</sup> revealed the presence of lateral (parallel to the substrate) and normal orientation of *n*-alkane molecules with respect to the NaCl(001) substrate, dependent on the *n*-alkane chain length and substrate temperature.

### **Epitaxial Growth Modes:**

Lattice matching and mismatching are the key factors for epitaxial growth. Film morphology and growth modes are directly related with each other. There are three standard models, **Frank-van der Merwe (FM)** growth (2D model), **Volmer-Weber (VW)** growth (3D model), and **Stranski-Krastanov (SK)** growth (mixed 2D and 3D model) for inorganic thin film growth on surfaces.<sup>24</sup>

In the FM model, the strong interaction between the deposit and the substrate leads to the uniform layer-by-layer growth on the substrate surface. In the VW model, the weak interaction between the deposit and the substrate leads to the nucleation of small clusters on the substrate. These nucleating sites grow into islands which further coalesce to form a non-uniform film. The VW growth sometimes shows high mosaicity of the material within the layer. The SK model utilizes the concepts of the FM and VW growth models and it is intermediate between the FM and VW growth modes.<sup>25</sup> In the initial stage of deposition a uniform film can be obtained which could later be covered with the 3D nucleating sites and clusters. Figure 1(a) presents the FM

model in which layer-by layer growth on a substrate is preferred. Figure 1(c) shows island growth of deposit on a substrate, due to comparatively weak interactions and Figure 1(b) shows the combination of both FM and VW models.

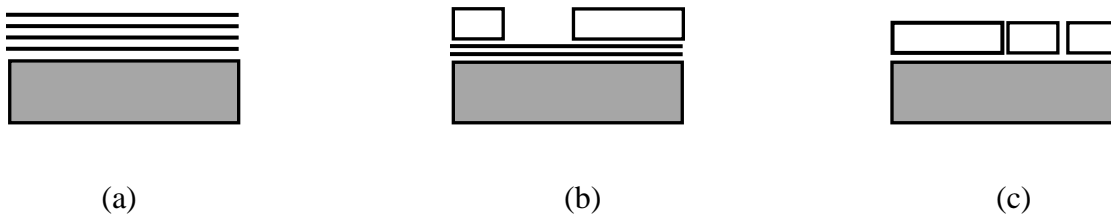


**Figure 1.1:** Different growth modes observed during epitaxial growth (a) layer-by-layer, Frank-van der Merwe growth (2D model), (b) layer-plus-island, Stranski-Krastanov growth (2D and 3D model), (c) island structures, Volmer-Weber growth (3D model). This figure is derived from reference 2.

### Substrates for Epitaxial Growth of Organic Molecules:

In the last few decades, various inorganic and organic substrates have been used for the epitaxial growth of organic molecules. Different substrates like Si(111), NaCl(110), KCl(110), MoS<sub>2</sub>, highly oriented pyrolytic graphite, HOPG(0001), and mica have been widely used substrates. On NaCl(001), *n*-alkane molecules align along the rows of sodium cations (the  $\langle 110 \rangle$  and  $\langle \bar{1}10 \rangle$  axes) due to favorable Columbic and van der Waals interactions in this geometry and film show 4-fold symmetry.<sup>23</sup> A freshly cleaved graphite surface has a tendency to grow alkane films epitaxially.<sup>7</sup> In epitaxial growth, *n*-alkane molecules follow the lattice structure of graphite and show 6-fold symmetry. These films can be grown with the alkane orientation in parallel or normal to the substrate plane, which depends upon the substrate temperature during film growth and the method of film preparation.<sup>20</sup>

#### 1.1.2 Techniques for the Preparation of Epitaxial Thin Films

Different techniques are used for growing epitaxial films. Pulsed laser deposition,<sup>20</sup> chemical vapour deposition<sup>21</sup> and molecular beam deposition<sup>23</sup> are commonly used techniques for inorganic thin film deposition. Physical vapour deposition (PVD) is a suitable technique for growing organic thin films. Different parameters like the deposition rate, film thickness and the substrate temperature can be manipulated.<sup>24</sup> Moreover, this technique has a wide application for the deposition of *n*-alkane thin films on different substrates.

### 1.1.3 Molecular Orientation and the Mechanism of Epitaxial Growth

Topography,<sup>21</sup> surface cleanliness, deposition rate<sup>24</sup> and substrate temperature<sup>7</sup> are key factors in determining the orientation of *n*-alkane molecules. On the basis of the work of Kubono *et al.*<sup>26</sup> two types of molecular orientation were observed during the thin film growth; one orientation was parallel and the other was normal to the substrate. These orientations can be understood from Figure 1.2.



**Figure 1.2:** Orientation of linear organic molecules on a substrate (a) In plane or parallel orientation of *n*-alkane molecules. (b) Normal or vertical orientation of *n*-alkane molecules. The long axis of the *n*-alkane is represented by a straight line.

During the film formation process, molecule-substrate and molecule-molecule interactions are present. Mainly, the van der Waals forces play a vital role for interacting hydrocarbon chains on

the substrate surface.<sup>23</sup> Long chain *n*-alkane molecules have strong interaction forces with the substrate which are responsible for the parallel orientation of alkane molecules. On the other hand, short chain *n*-alkane molecules have weaker interactions which results in a normal orientation for these molecules on substrate surface.<sup>23</sup> It was observed that supercooling is a crucial factor for determining the lateral and normal orientation during the epitaxial growth.<sup>26</sup> Supercooling can be defined as the difference between the melting temperature of the sample and the substrate temperature during deposition ( $\Delta T = T_{\text{sample}} - T_{\text{substrate}}$ ).<sup>27</sup>

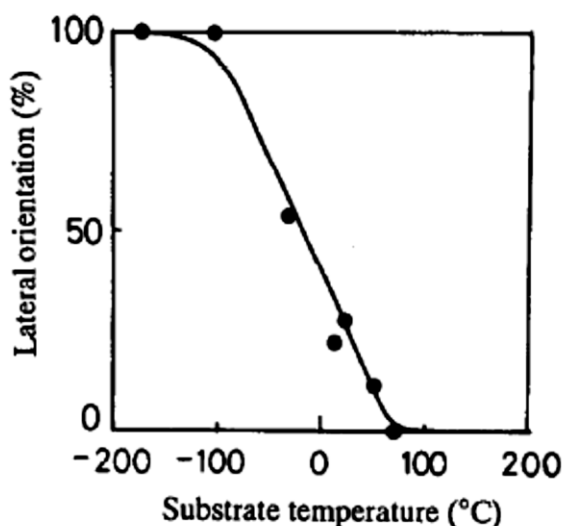


**Figure 1.3:** Plot of lateral orientation fraction of  $C_{40}H_{82}$  thin film against the substrate temperature ( $^{\circ}C$ ). This figure is reprinted from reference 26 with permission.

Figure 1.3 presents the lateral molecular orientation at different substrate temperatures. If the deposition process occurs at higher substrate temperature (lower supercooling) then the percentage of *n*-alkane molecules with lateral orientation will be lower. On the contrary, when deposition occurs at lower substrate temperature (higher supercooling) then the percentage of laterally oriented molecules will be higher.<sup>26</sup>



Tanaka *et al.*<sup>27</sup> postulated that during the adsorption-desorption process among different vibration modes, the precessional rotation of molecule around its main axis leads to normal orientation. Saito *et al.*<sup>28</sup> examined the film growth mechanism when films of stearic acid were deposited on a KCl substrate, and observed that the adsorption energy was directly related to the chain length and the growth rate of molecules with a normal orientation was higher than for molecules with a parallel orientation.

The detailed mechanism of orientation was proposed by Kubono *et al.*<sup>29</sup> In this model (Figure 1.4), it was assumed that the adsorbed long chain molecules acted as anisotropic rigid rods in clusters, in the vapour phase and in the first step of adsorption these acted as free moving long chain molecules. The vapour molecules reaching the substrate can migrate along the substrate to achieve their minimum energy state (clusters) or re-evaporate from the substrate. The re-evaporation rate depends on the substrate temperature, molecular orientation and the interaction energy between the organic molecules and the substrate. The stronger the deposit-substrate interactions the slower the rate of re-evaporation.

Therefore, during film growth the shorter chain alkane molecules will re-evaporate faster relative to longer chain molecules. At lower substrate temperature, normal oriented molecules will re-evaporate faster due to the small population of normal oriented molecules, while at higher substrate temperature, the clusters of laterally oriented molecules evaporate faster due to their higher relative area, which result in higher population of normally oriented molecules.<sup>29</sup>

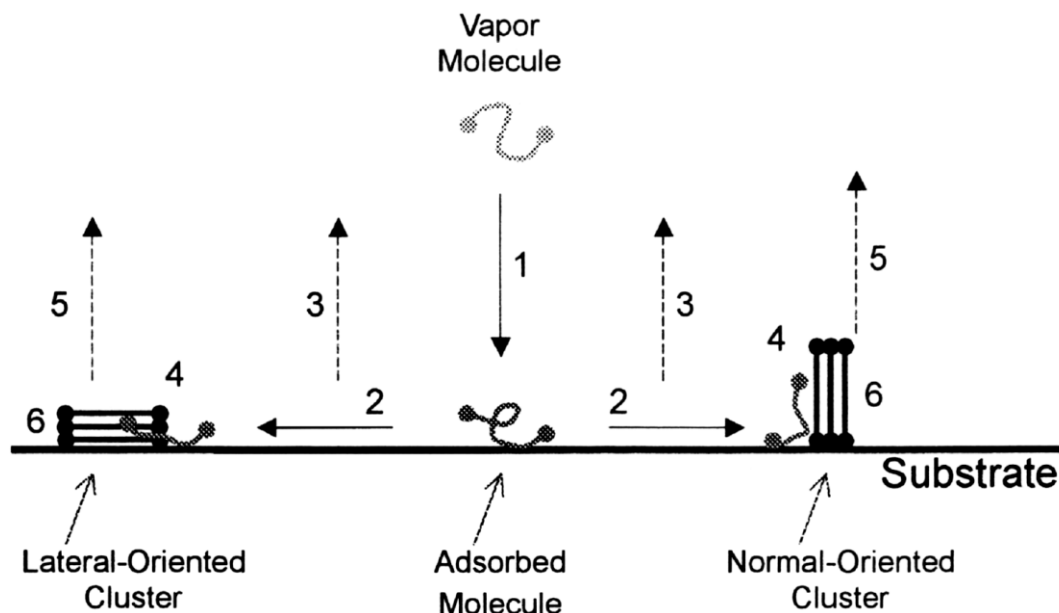


**Figure 1.4:** Thin film formation on a substrate. (1) adsorption from vapour, (2) migration, (3) re-evaporation from substrate, (4) cluster formation, (5) re-evaporation from cluster, (6) reorientation. This figure is reprinted from reference 29 with permission.

On the basis of the above model it was shown that the molecular orientation depends on the relative re-evaporation rate and the strength of the deposit-substrate interactions.

## 1.2 Orientation Control in Thin Films and its Importance

Organic thin film based electronic devices are getting considerable attention due to their often potentially useful electronic, optical and chemical properties.<sup>5,30</sup> These properties are directly related to the molecular orientation in the organic thin films. Molecular level orientation control in the organic thin films is an important factor in the successful development of commercial molecular devices.<sup>31-33</sup> The chemical and physical properties of these films are directly related to the molecular functionality, ordering, orientation, and surface morphology.<sup>25,34</sup>

Vacuum evaporation is an effective technique for obtaining highly ordered organic thin films.<sup>28,29</sup> The morphology and molecular orientation of the vacuum deposited organic films can be modified by controlling deposition conditions such as substrate temperature,<sup>28</sup> deposition

rate,<sup>26</sup> and length of the molecular chain in case of *n*-alkanes.<sup>7,28</sup> For a given chain length it was suggested that the substrate temperature is the most significant factor for the determination of molecular orientation in thin paraffin film.<sup>26</sup>

There are a number other factors such as field effects and the substrate crystal orientation that can play a crucial role in the orientation of molecules on the substrate. An intrinsic complexity with organic thin films is the short range ordering and presence of defects.<sup>29,35</sup> These problems could be reduced by an applying additional external effect such as magnetic or electric field,<sup>36</sup> a temperature gradient,<sup>7</sup> and some other surface interactions. The application of an electric field to thin films of diblock copolymers causes domain alignment as well as long range molecular ordering.<sup>36-38</sup> When a thin diblock copolymer were restrained between two electrodes and heated above its glass transition temperature, the micro domains become oriented in the direction of the electric field as shown in the Figure 1.5.<sup>38</sup>

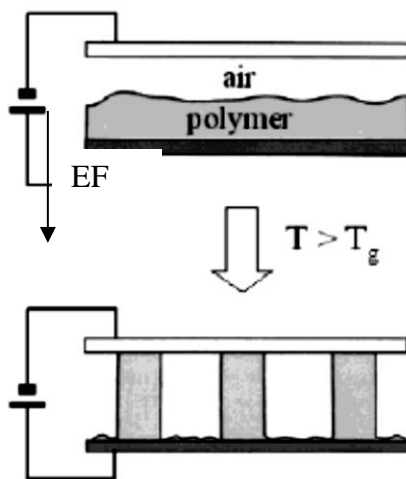


**Figure 1.5:** Schematic of the experimental set up for electrical field induced patterning in diblock copolymer films. This figure is reprinted from reference 38 with permission.

Hatashi *et al.*<sup>39</sup> applied an electric field of 1 V/ $\mu$ m during the epitaxial growth of copper phthalocyanine thin films on KCl(001) substrate. The result showed some molecular alignment in the direction of the electric field. However, the mechanism of electric field induced orientation was not clear. Molecular orientation of organic LC molecules can also be controlled by applying an electric field.<sup>40,41</sup> Unlike polymer films, orientation of LC molecules does not require a high electric field.<sup>38</sup> Even under the application of weak electric field the LC molecules can be aligned in the direction of electric field. However, after removing the electric field the molecule randomize their orientation.<sup>42</sup>

Paineau *et al.*<sup>43</sup> were able to align clay sheets parallel to a magnetic field and perpendicular to the electric field. In the process, highly patterned structures were obtained. Papadantonakis *et al.*<sup>44</sup> determined that the *n*-alkane solutions such as C<sub>29</sub>H<sub>60</sub>, C<sub>33</sub>H<sub>68</sub> and C<sub>37</sub>H<sub>76</sub> in phenyl octane can act as a template for controlling the orientation of monolayers of an alkyl ether of same molecular chain length.

### 1.2.1 Orientation Control Using LC Imprinting

#### LC and LC Phases

Liquid Crystal (LC) is a median phase between the solid and liquid phase. There are two types of LCs, lyotropic LCs and thermotropic LCs.<sup>45</sup> Lyotropic LCs are formed when some amphiphilic molecules are dissolved in a solvent (water) at different concentrations.<sup>46</sup> Surfactants are the example of lyotropic LCs.<sup>45</sup> Thermotropic LCs are temperature dependent and are formed by heating anisotropic organic molecules. Anisotropy is a directional dependent property and the molecular orientational order can be influenced with the help of external fields.<sup>45</sup> In the proper phase LCs have a natural ability to respond to a low electric field, in comparison to solids,

liquids and gases which show little response even with a strong electric field. LC molecules possess some orientation order depending upon the phase of the LC.<sup>45</sup>

When a magnetic or electric field is applied to a LC film the different phases of the LC will show a different response, characterized by their director (the average direction of all the molecules).<sup>45</sup>

An example of a thermotropic LC is 8CB (4-octyl-4-cyanobiphenyl).<sup>46</sup> Thermotropic LCs are particularly popular due to their use in liquid crystal displays (LCD).

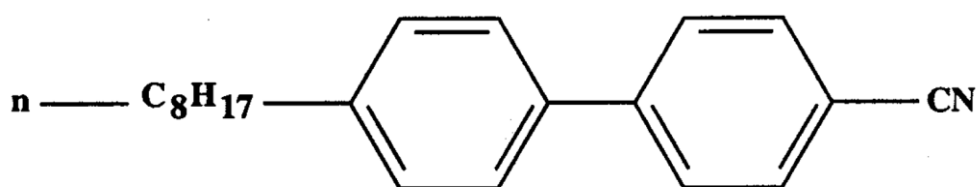


**Figure 1.6:** Structure of LC, 8CB (4-octyl-4-cyanobiphenyl) molecule.

Thermotropic LCs exhibit nematic, isotropic, smectic and cholesteric phases. In the nematic phase,<sup>46</sup> the LC rod-like molecules have less positional order but tend to align in the same direction. In the smectic phase,<sup>46</sup> the rod-like molecules have a layered arrangement and these molecules tend to align in the same direction (Figure 1.7). The molecular motions are constrained within the layers and have more orientation order. In the isotropic phase,<sup>46</sup> the rod-like molecules are randomly oriented with no long range orientation order. The term cholesteric phase is related with cholesterol containing LCs.<sup>46</sup>

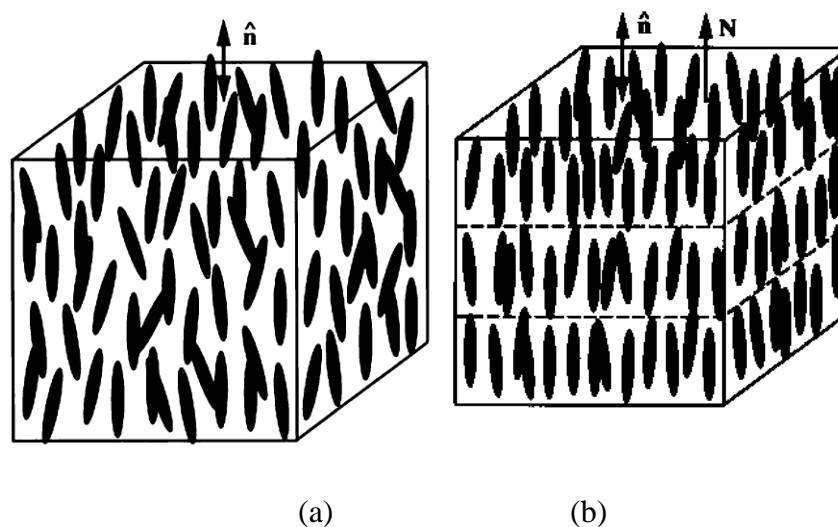


**Figure 1.7:** (a) Nematic phase of LC (b) Smectic phase of LC, the vector  $\hat{n}$  represents the director of the LC molecules. This figure is reprinted from reference 46 with permission.

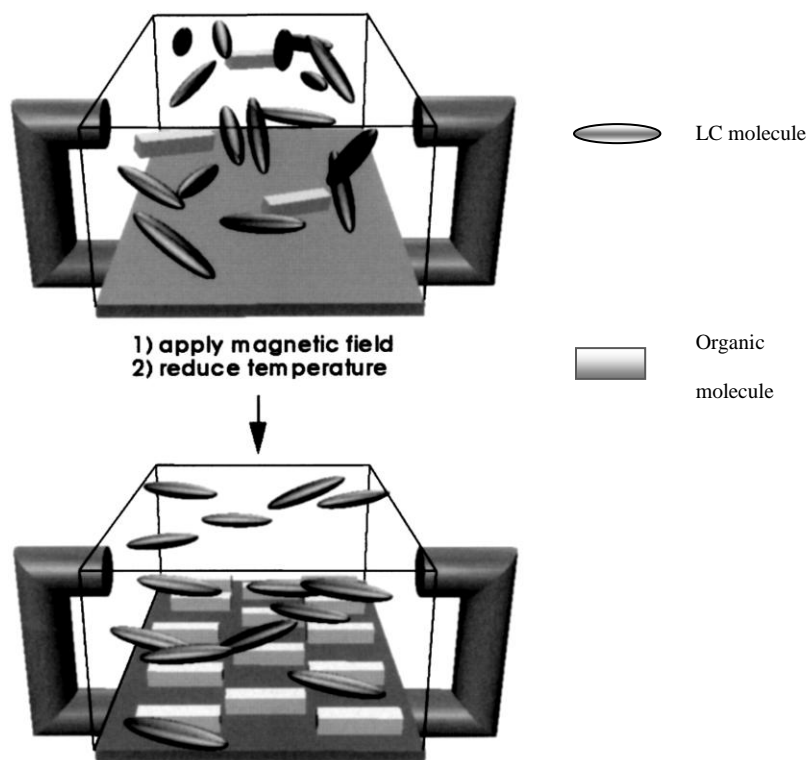
### Orientation Control using LC:

A LC can be used to control the orientation of organic molecules.<sup>47,48</sup> The Patrick group (Western Washington University, USA) has been working to use the LCs for controlling the molecular orientation of organic molecules over the past decade. A brief outline of their work is mentioned here.

Lynch and Patrick<sup>47</sup> were successful in obtaining highly oriented carbon nanotubes by orienting LC solvent on a highly grooved polycarbonate substrate. Copper electrodes were deposited on the substrate and an electric field of  $1.8 \text{ V}\mu\text{m}^{-1}$  was applied for LC orientation. During the process, an external field aligned the LC molecules which in turn aligned the carbon nanotubes. The LC drained out through grooves on the polycarbonate surface.

Mougous *et al.*<sup>48</sup> worked to control the orientation of organic molecules in thin films by using Liquid Crystal Imprinting (LCI). In this technique, the LC film is initially oriented by applying a strong magnetic field while it is simultaneously heated. Then, a thin film of organic molecule is deposited on the oriented LC film. During the process, the aligned LC molecules act as a

template for orienting the organic thin film. A mixed layer of *n*-tetracosanoic acid (TA) and 8CB was aligned uniaxially with the help of 8CB (LC) solvent in the presence of an external magnetic field of few KGauss.



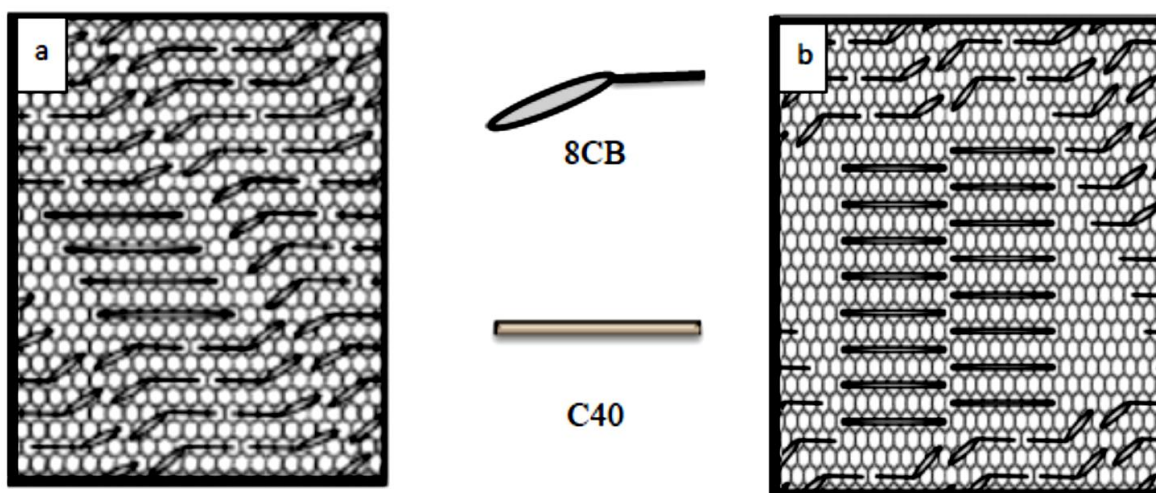
**Figure 1.8:** Liquid Crystal Imprinting (LCI) in which LC molecules are aligned parallel to the applied magnetic field and these LCs act as a template layer for aligning subsequently deposited organic molecules. This figure is reprinted from reference 48 with permission.

Figure 1.8 illustrates the LCI technique. Initially, a layer of LC molecules is aligned parallel to the applied magnetic field, while in the organic deposition step the organic molecules replace the LC molecules, maintaining the LC orientation.

Further investigation was done to verify the LC template effect using the LCI technique with a fluorescent dye 3-(2-benzothiazolyl)-7-octadecyloxy coumarin (BOC) on HOPG. When a film of dye molecules was deposited on top of oriented 8CB, orientation control was observed in the dye

molecules. However, when the same experiment was repeated with 1-phenyl octane, no orientation control was observed within the fluorescent dye molecular film.<sup>49</sup>

Another method was also adopted to control the orientation of a monolayer of *n*-alkane by using an oriented LC film. A film of LC (8CB) was prepared on a freshly cleaved HOPG surface while a magnetic field of 1.2 Tesla (T) was applied parallel to the substrate. In the next step, a drop of a saturated solution of *n*-tetracontane ( $C_{40}H_{82}$ ) mixed with 8CB was applied on top of the oriented LC film. The sample was then heated for few minutes in a heating oven. When this sample was studied by STM, a highly oriented monolayer of *n*-alkane with the same LC orientation was observed.



**Figure 1.9:** Proposed model by Patrick's group in which LC (8CB) molecules are replaced by C40 molecule. Initially 8CB is oriented parallel to the magnetic field. This image is reprinted from reference 1 with permission.

In Figure 1.9 the process of C40 alignment by the sacrificial template behavior of the LC film is illustrated. It is shown that the two LC molecules lie down on the substrate in such a way that their long axis (alkyl chain) are facing each other and are parallel to substrate.<sup>1</sup> Initially, a strong



magnetic field was applied parallel to substrate and it helped to orient the LC molecules in a single direction. Afterwards, C40 was deposited by the solution casting method from a saturated solution of *n*-alkane. During the deposition process, every two molecules of LC were replaced by one molecule of C40.<sup>1</sup> As a result, an oriented *n*-alkane monolayer was observed by STM. The effect of magnetic field for the orientation of the LC molecules is discussed in the following section.

### **1.2.2 Effect of Magnetic Field on LC Orientation**

According to Chandrasekhar,<sup>50</sup> when a magnetic field is applied to the LC molecules the LC molecules will tend to align along or against the field. When an external magnetic field is applied to the LC molecule film, an induced magnetic dipole can be produced.<sup>45</sup> The magnetization (induced magnetic dipole) of LC molecules also depends upon the phase of the LC. If the magnetization value of LC molecules is high then a small magnetic field will be enough to orient the LC molecules. There are certain threshold values for orienting the LC molecules depending upon the phase of a LC. The threshold magnetic field for orienting a 25 micrometer thick LC film is 0.2 T.<sup>45</sup> A magnetic field of 1.2 T was enough to orient a LC monolayer on a graphite substrate.<sup>1</sup>

### **1.2.3. Effect of Electric Field on LC Orientation**

The response of a LC towards an electric field is important for industrial applications.<sup>45</sup> The ability of LC molecules to align along the external field is caused by the dipole moment of the molecules. A permanent electric dipole arises when one end of the molecule has positive and the other end has a negative charge on it.<sup>45</sup> When an external field is applied to the LC, the dipole molecule will tend to orient along the direction of the field as shown in Figure 1.10. Even if the molecule does not have a permanent dipole, it can still be influenced by an electric field.<sup>48</sup>

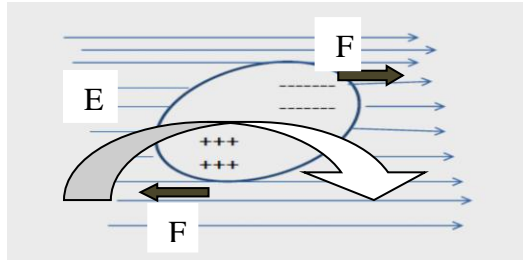


**Figure 1.10:** Effect of electric field on the orientation of LC molecules. This figure is derived from reference 45. The blue arrows represent the electric field vector (E) while the black arrows show the electric force (F) on the molecule.

A thin film is represented by a collection of polar molecules in the Figure 1.11. All the molecules have positive charges on one end and negative charges on the other end. The charge separation in LC molecular film shows electric dipole. If the molecular dipole moment has the same direction as the long molecular axis then its dielectric constant is said to be positive  $\Delta\epsilon > 0$ . A small electric field is required to orient the LC molecules having a large dielectric constant value.<sup>45</sup>

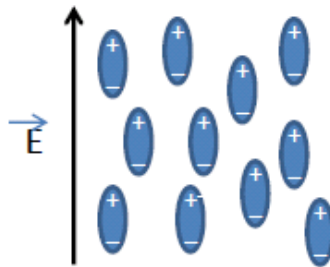


**Figure 1.11:** Behaviour of molecules with positive dielectric constant value in an electric field. This figure is derived from reference 45.

On the other hand, LC molecules with a dipole moment perpendicular to the long molecular axis have negative dielectric constant  $\Delta\epsilon < 0$ , and their orientation tends to be perpendicular to the electric field. 8CB has a value of  $\Delta\epsilon = 6.15$  and a molecule with a large dielectric constant

requires a small electric field to orient the molecule,<sup>52</sup> for example a 25  $\mu\text{m}$  thick nematic LC film requires a 400 V/cm electric field to orient the LC film on a glass substrate.<sup>45</sup>

### 1.3 Research Approaches

The main focus of this project is to develop methods to control the orientation and ordering of molecules in epitaxially grown organic thin films. As a first step of work, the magnetic field LCI technique of the Patrick group was reproduced. Their work focused on orientation control of an *n*-alkane monolayer, but in this work the alignment of an *n*-alkane multilayer thin film was examined. The experimental conditions were optimized to reproduce the results for this system. The detailed results of these experiments are discussed in Chapter 4.

A new approach was developed by modifying the LC orientation process. Instead of a magnetic field, an electric field was used to orient a LC film on NaCl(001) substrate. Then, thin films of the *n*-alkane were grown epitaxially by PVD process on the oriented LC. Highly oriented *n*-alkane thin films were obtained by the sacrificial template act of LC. The detailed results are discussed in Chapter 4.

## CHAPTER 2

### EXPERIMENTAL APPARATUS

During the course of this research work, several different experimental apparatus were used. For the first set of experiments a specially designed heating cell was constructed for the magnetic alignment of a LC film. This heating cell was used to reproduce the results obtained for the magnetic alignment by LCI technique for oriented *n*-alkane films. Dipole magnets were used to apply a high magnetic field and the *n*-alkane films were subsequently grown by PVD. The characterization of thin films was done by polarized optical microscopy. For the second phase of the research, LC orientation was done by applying an electric field to a LC thin film on a NaCl(001) substrate. *N*-alkane thin films were subsequently grown by PVD on the oriented LC film and samples were characterized by optical microscopy. All experimental apparatus used during the research and the working of these instruments are described in this Chapter.

#### 2.1 Heating Cell

A specially designed heating cell was constructed for holding and heating the sample during the first set of experiments in which a magnetic field was applied for LC orientation. The heating cell held the sample in a fixed position in the strong magnetic field. The heating cell was made up of a non-magnetic material so that it was not attracted to the magnets. The heating cell was also thermally isolated from the magnets. The Physics Department machine shop helped with the construction of the heating cell.

##### **Construction of heating cell holder:**

An aluminum metal block was cut into a rectangular shape 17 mm wide. At one end, a hole of 15 mm deep and 2.5 mm diameter was drilled, to match the diameter of the heater. A 120 V

cartridge heater was purchased from Canadian Tire. This heater was controlled with the rheostat (Standard Electrical Products Co., Dayton, Ohio, USA). The temperature of the heating block was monitored with a K-type thermocouple by attaching the tip of thermocouple to the surface of the aluminium block. Ceramic plates were attached to the both sides of heating cell, to avoid excessive heat transfer to the dipole magnets.

A smaller size heating cell/holder with  $\frac{1}{2}$  the width of the previous cell was also designed to work with a smaller magnetic pole separation, to provide a strong magnetic field. Both heating cells are shown in Figure 2.1

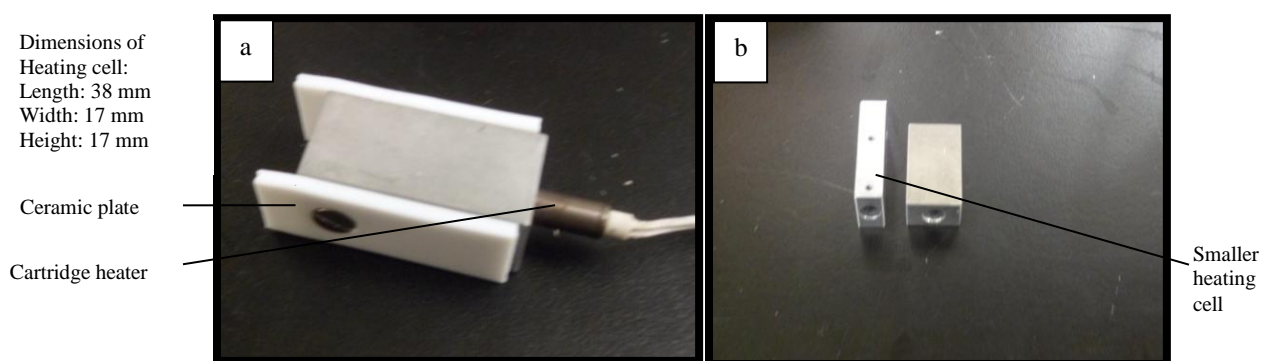


**Figure 2.1:** (a) Heating cell with heater and ceramic thermal plates isolation. (b) Two different sizes of heating cells.

## 2.2 High Field Dipole Magnets for Sample Alignment

During the experiment, the LC molecules were oriented by applying the magnetic field in the plane of the substrate. Initially, the **Bruker EMX EPR** spectrometer from the Saskatchewan Structural Science Centre (SSSC) at the University of Saskatchewan was used. This EPR spectrometer has a maximum magnetic strength of 1.0 Tesla (10 KGauss). The cavity inside the pole face has a uniform magnetic field and the strength of magnetic field was tuned by software. This instrument is shown in Figure 2.2.

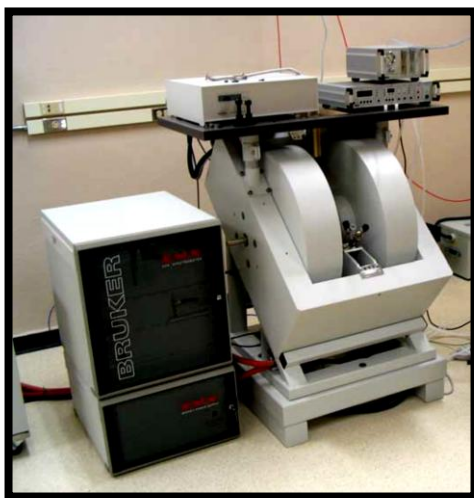


**Figure 2.2:** Bruker EMX-EPR Spectrometer in the Saskatchewan Structural Science Centre (SSSC).

It was found that the experiment required a yet stronger magnetic field. Thus, a stronger dipole magnetic system, **Danfysik System 8000**, from Canadian Light Source (CLS) magnet mapping lab was used. This dipole magnet can go to a magnetic field strength of 3.0 Tesla (T). These magnets were manually controlled and a Tesla meter (Figure 2.4) was used to verify the magnetic field strength. A magnetic field of 2.33 T was used while working with the smaller heating cell. During the experiment this heating cell was placed so that the magnetic field was aligned in the plane of the sample. This instrument is shown in Figure 2.3.

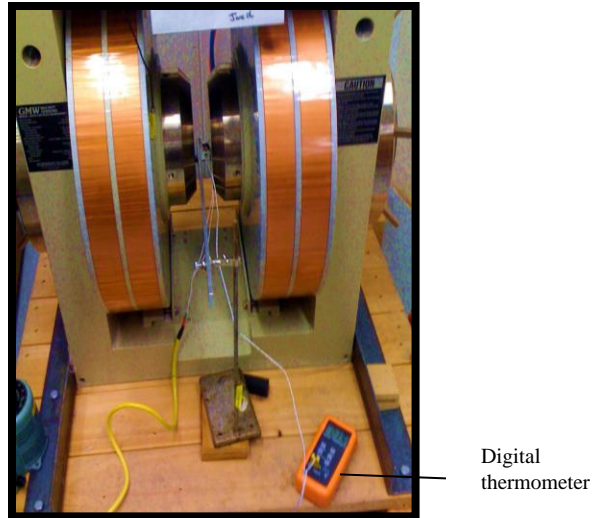


**Figure 2.3:** Experimental setup for magnetic field alignment using Danfysik system 8000, magnetic system in magnet mapping lab (CLS).

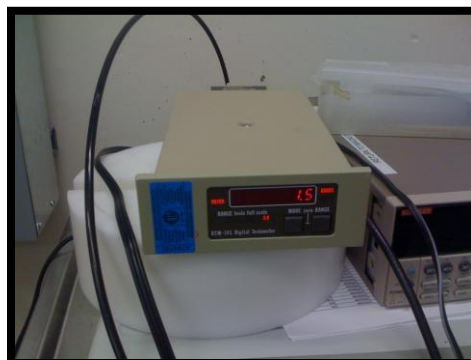


**Figure 2.4:** Teslameter for measuring magnetic strength from magnet mapping lab (CLS).

The magnetic field strength was correlated with the gap distance between the magnet poles. The following plot shows the relationship between the magnetic field strength (T) and the gap (mm) between the pole faces for this magnet.

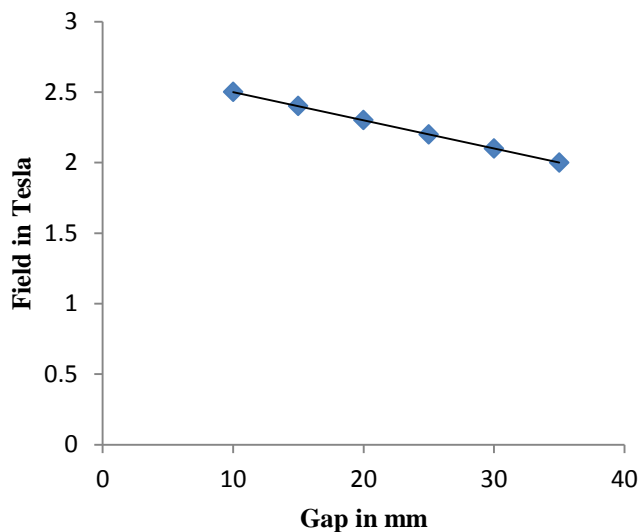


**Figure 2.5:** Plot of the relationship between pole face gaps (mm) and magnetic field (T).<sup>53</sup>

From this plot it is obvious that if the gap between the pole faces is smaller, the magnetic strength will be greater. This graph was used to construct a smaller heating cell for higher field studies.

### 2.3 Evaporator for Physical Vapour Deposition

During these experiments, thin films of the *n*-alkane were deposited on various substrates (graphite, NaCl) having a magnetically oriented LC layer. *N*-alkane films of uniform thickness were grown by PVD in vacuum ( $10^{-7}$  Torr). A resistivity heated tungsten boat was used to hold the *n*-alkane sample for evaporation. A specially designed substrate holder with a Peltier heater to heat the substrate, was  $\sim 15$  cm above the evaporator boat. A quartz-crystal microbalance, located just beside the substrate holder, was used to monitor the sample thickness and deposition rate during deposition. A temperature controller (TE Technologies, USA) was used to measure and control the temperature of substrate during deposition. A thermistor was used to monitor and regulate the temperature and was attached to the Peltier plate near the substrate. The deposition



rate was controlled by adjusting the current supply to the evaporator boat during the deposition process.



**Figure 2.6:** Vacuum evaporator

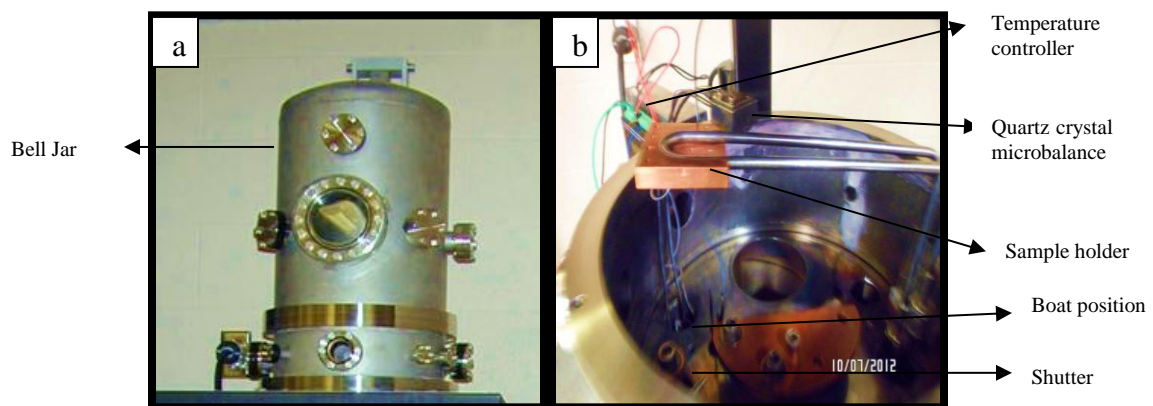


**Figure 2.7:** (a) Vacuum chamber external view. (b) Vacuum chamber internal view.

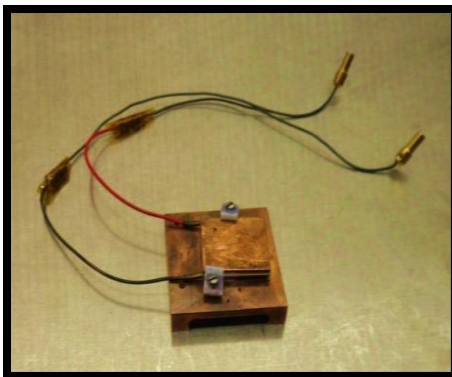


**Figure 2.8:** Sample holder with copper plate on top of Peltier heater.

Figure 2.7(b) presents different internal parts of vacuum chamber. Figure 2.8 shows the sample holder with copper plate and peltier heater.

## **2.4 Electric Field Alignment**

Electric field alignment of the LC was proposed as an alternate to magnetic field alignment. A special sample holder was constructed (described below) for the alignment of the LC thin films. The sample was placed between two electrodes which were about 1 mm apart.

## **2.5 Electrode Formation**

A  $\text{Si}_3\text{N}_4$  window was modified for holding the sample during electric field alignment. Two gold (70 nm thick) electrodes were deposited by PVD on both sides of the window, by covering the central portion of the window with a carbon tape.

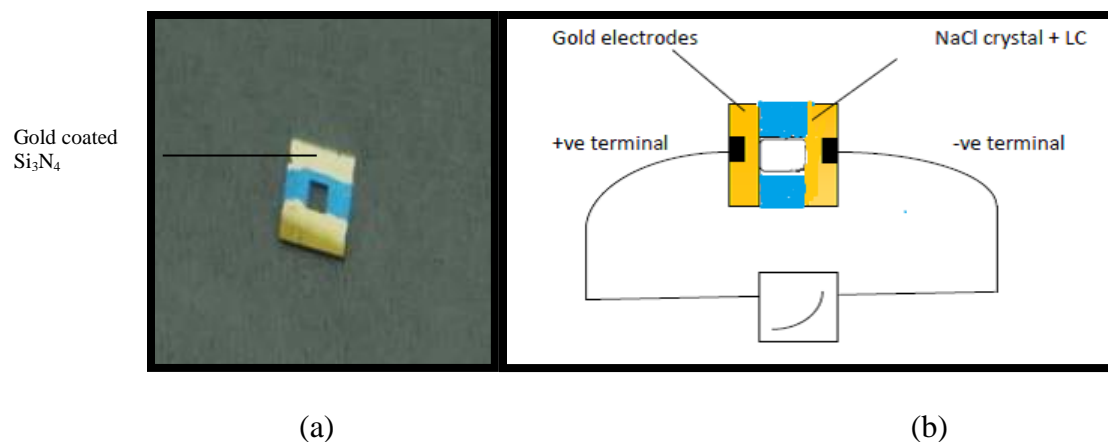


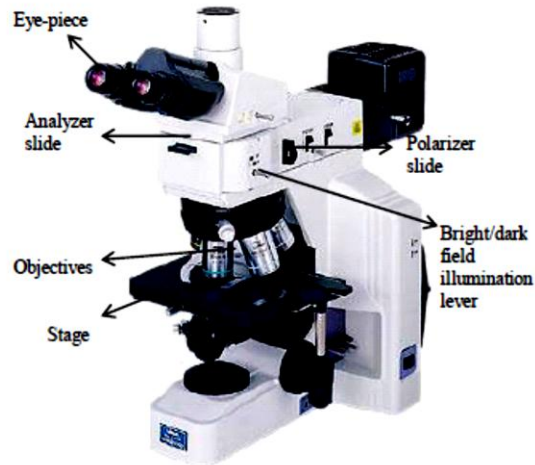
**Figure 2.9:** (a) 70 nm thick gold layer deposited on  $\text{Si}_3\text{N}_4$  window at room temperature by PVD. (b) Schematic diagram of the LC orientation experiment.

The schematic set up of electric field alignment process is shown in Figure 2.9(b), in which the sample (NaCl+LC) was placed between the electrodes. A DC voltage supply was connected to the gold electrodes during the LC orientation process. The sample was placed between the electrodes (1 mm separation) on a heating cell. A DC voltage of 20 V was applied to the sample during the experiment from a HP 6236B power supply. A thermocouple (K-type) was attached to the sample holder to monitor the temperature. After orienting the LC sample, a thin layer of C40 was deposited on top of the sample by PVD and sample characterization was done by optical microscopy.

## 2.6 Optical Microscopy

Optical Microscopy is a valuable instrument for investigating sample morphology down to the 0.5  $\mu\text{m}$  (micrometer) scale. A **Nikon Eclipse ME600** polarized optical microscope was used to study the structural changes of the sample during the experiments with the help of a digital camera. This optical microscope has objectives that can magnify the image from 5 X - 100 X, and a set of magnifying (10X) eye pieces. This microscope can magnify in the range 50X - 1000X. This microscope operates with epi-illumination in bright field (BF), dark field (DF)

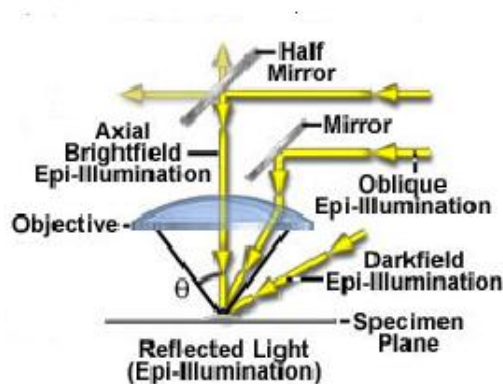
modes and polarized imaging. Optical microscopy can be helpful for research and development in the field of semiconductors, electronics, pharmaceuticals, general metallurgy, crystallography and ceramics by studying the sample morphology.<sup>54</sup> Figure 2.10 presents the different parts of an optical microscope.



**Figure 2.10:** (a) 70 nm thick gold layer deposited on  $\text{Si}_3\text{N}_4$  window at room temperature by PVD. (b) Schematic diagram of the LC orientation experiment.

### Epi-illumination:

Epi-illumination is defined as the “illumination from top of the sample surface.”



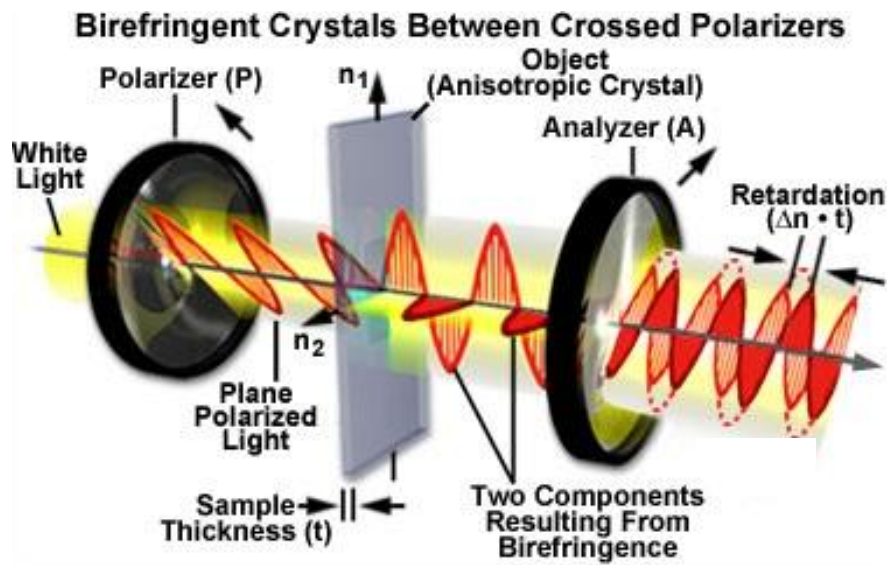
**Figure 2.11:** Schematic illustration of bright and dark field epi-illumination. This figure is reprinted from reference 55.

Figure 2.11 presents the phenomenon of epi-illumination, in which the light illuminates the sample from the top and the reflected light is used to form an image.<sup>56</sup> The phenomenon of epi-illumination is helpful to study the surface morphology, surface geometry and topography of the sample.<sup>55</sup> In bright field illumination, the sample is illuminated along the axis of the objective lens, normal to the sample surface.

In dark field illumination the light illuminates the sample at an angle. Some of the light is scattered if the sample surface is not even.<sup>56</sup> Dark field imaging is helpful for identifying the defects, dust and edges.

### **Polarized Light Microscopy:**

Most solid substances have optical properties these depend upon the polarization of incident light (anisotropy). When these materials are rotated, different color changes can be observed depending on the orientation of the material in the light path. These color changes can be useful to illustrate and identify various materials.<sup>57,58</sup> There are two polarizing filters in a polarized optical microscope. Initially, light passes through a fixed polarizer and is reflected by the sample. Then this light passes through the rotatable analyzer. Only the light with polarization parallel to the polarization of the rotatable analyzer can pass through it. Polarized optical microscopy helps in enhancing contrast for the birefringent materials and to differentiate between isotropic and anisotropic materials. The position of the polarizer and the analyzer in the microscope is shown in Figure 2.12.



**Figure 2.12:** The effect of birefringent sample and polarizers in the transmission of light. This figure is reprinted from reference 57.

## CHAPTER 3

### EXPERIMENTAL WORK

The first goal of this research work was to reproduce the results of the Patrick group for the growth of oriented *n*-alkane thin films using a magnetically oriented LC template film. The second part of this research work was to modify and extend the concept of LC orientation by using an electric field to obtain a highly oriented *n*-alkane thin film. The detailed experimental setup for this work is explained in this Chapter.

### 3.1 Orientation Control by Magnetically Oriented LCI

#### 3.1.1 Experimental Approach

Freshly cleaved Highly Oriented Pyrolytic Graphite (HOPG), ZYH-grade was used as a substrate. Thin films of LC (8CB) were prepared by placing a 1  $\mu$ L drop of LC on a clean HOPG surface. These films were heated to 100 °C for 2-3 minutes in a specially designed heating cell in a strong magnetic field oriented in the plane of the substrate. The sample was then cooled to room temperature within the magnetic field. Subsequently, a thin film of C40 was deposited on the LC surface by physical vapour deposition. A polarized optical microscope was used to examine the samples after the deposition.

#### 3.1.2 Sample Preparation

##### 3.1.2.1 *N*-Alkane and LC Candidates

The *n*-alkane used for this project was *n*-tetracontane ( $C_{40}H_{82}$ , C40) with 97% purity purchased from Alfa Aesar. DSC (Differential Scanning Calorimetry) was used to verify the purity of the compound. The melting point of C40 and LC samples were determined by TA Instrument, DSC Model 220 from the Physical Chemistry undergraduate laboratory (University of Saskatchewan). Figure 3.1 presents the DSC scan of the C40 sample.

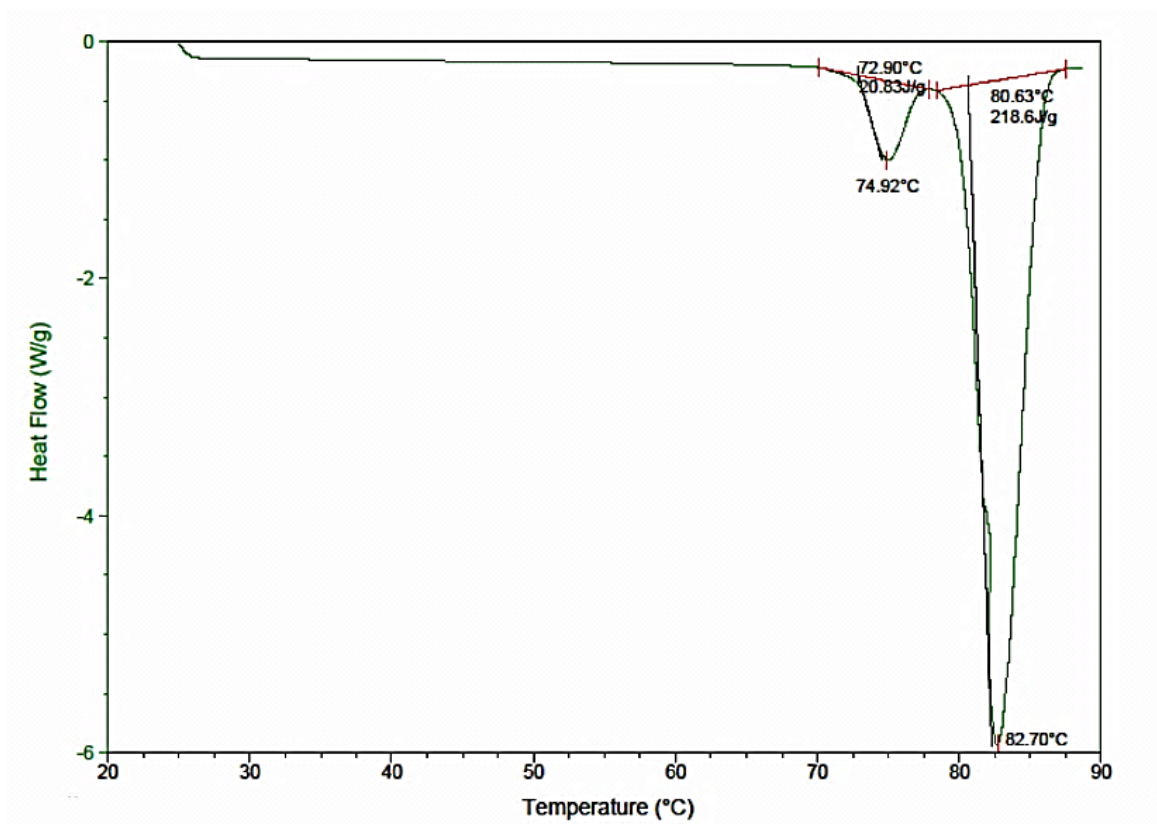


**Figure 3.1:** DSC spectrum of *n*-tetracontane.

From the DSC curve, a melting point of 82.7 °C was obtained which was close to literature value<sup>59</sup> as shown in table 3.1. LC (8CB) (4-octyl-4-cyano biphenyl), (Smectic-Anisotropic phase transition: 21.5 °C; Anisotropic-Nematic phase transition: 33.5 °C; Nematic-Isotropic phase transition: 40.5 °C)<sup>1</sup> was purchased from Frinton Laboratories USA, with 99% stated purity. A DSC scan was done to verify the purity of the compound. The DSC scan is presented in Figure 3.2. Only one transition phase of LC sample was detected and its value was close to the literature value.<sup>1</sup> No purification was performed for the *n*-alkane and LC samples. Table 1 compares the melting point values of these compounds with the literature value.



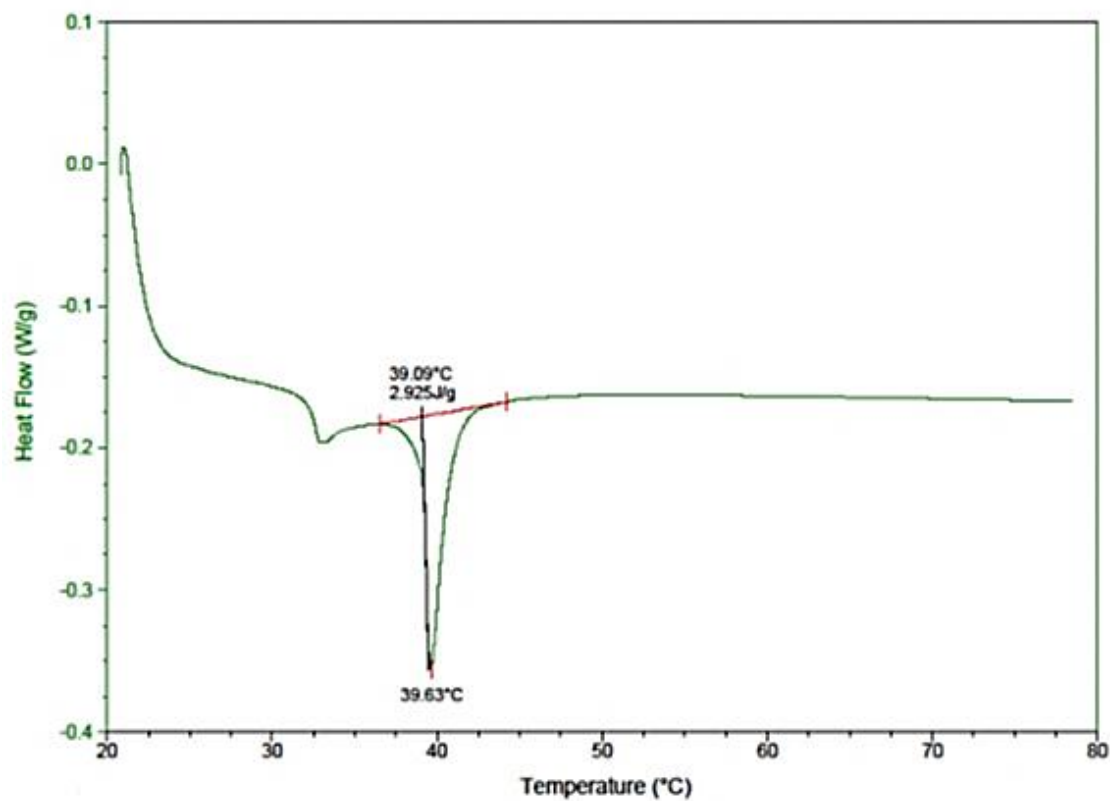


**Figure 3.2:** DSC spectrum of 8CB (4-octyl-4-cyanobiphenyl).

Compounds	Phase Transition	Literature Values	DSC Values
$C_{40}H_{82}$	Melting Point	81.5 °C <sup>59</sup>	82.7 °C
8CB	Nematic-Isotropic	40.5 °C <sup>1</sup>	39.6 °C

**Table 1:** Comparison of phase transition values among literature and DSC values.

### 3.1.2.2 Substrate Selection

For epitaxial growth of *n*-alkane films many substrates can be used, as discussed in Chapter 1. For these experiments HOPG(0001) (10 x 10 x 2 mm, ZYH-grade) was used as a substrate. This was purchased from NT-MDT Co. (Russia), and was used without further purification. Some samples were also prepared by using Natural Kish Graphite (grade 300) from Graphene Supermarket, (USA) for comparison.

There are two different methods to mount graphite as a substrate.

(1) Highly Oriented Pyrolytic Graphite (HOPG-ZYH grade) was washed with Acetone (~99.9%) and Ethanol (99.9%). These substrates were dried by placing the graphite in the heating oven at 120 °C for 5 minutes. The top layers of HOPG were then cleaved with scotch tape to expose a fresh surface. The fresh HOPG surface was used as a substrate.

(2) Another HOPG substrate was prepared on a fresh, clean Silicon (Si) surface (1 x 1cm). Initially, a flake of Kish graphite was peeled many times with scotch tape to get an extremely thin graphite film. This film was applied to the Si wafer by rubbing the tape on top of the Si surface.

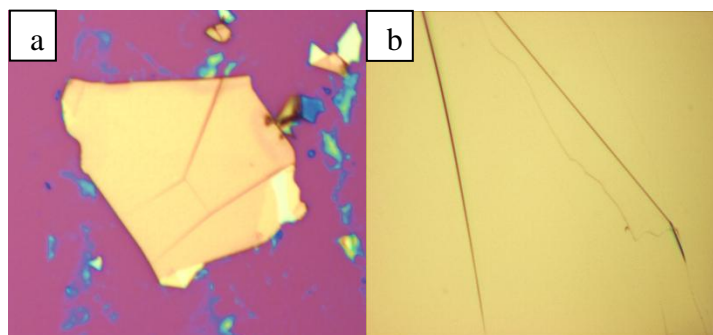


**Figure 3.3:** Polarized optical microscope images of the samples having (a) freshly peeled Kish graphite on a clean Si(111) surface. (b) freshly cleaved HOPG surface, at 50X objective lens magnification and bright field illumination.

Figure 3.3 presents the freshly cleaved graphite mounted on Si substrate and freshly cleaved HOPG.

### **3.1.2.3 LC Film Preparation and its Alignment**

LC films were prepared by using a pure LC and a diluted LC solution. The LC solution was prepared by dissolving pure ethanol (99.9%) with the LC (8CB) in a 50:1 ratio. Following is the approach which was adopted for aligning LC films in a magnetic field.

**Step 1:** A drop (200 $\mu$ L) of pure or diluted LC (8CB) was placed onto the freshly cleaved graphite surface with a micropipette. Ethanol from the diluted 8CB was allowed to evaporate.

**Step 2:** The HOPG sample (with either diluted LC or pure LC on its surface) was mounted on the heating cell. The heating cell was heated from room temperature to 100 °C, and the sample was held at 100 °C for 1 minute in the fixed magnetic field, oriented in the plane of the substrate.

**Step 3:** The sample and heating cell were allowed to cool to room temperature, within the magnetic field

**Step 4:** Samples were examined by the polarized optical microscope with 100X objective lens magnification with bright field illumination. These results are present in Chapter 4.



**Figure 3.4:** Position of sample within the dipole magnets in magnetic mapping lab (CLS) during the alignment experiment.

Figure 3.4 shows the position of the substrate and sample holder within the dipole magnets. A sample holder was designed for holding samples within the poles of magnets while heating. The detailed description of these experimental apparatus is found in Chapter 2. This procedure was also applied for making a sample in the absence of a magnetic field.

#### **3.1.2.4 C40 Deposition by Solution Casting**

For C40 deposition, a solution casting method was initially adopted for the epitaxial growth of *n*-alkane thin films, based on the method used by the Patrick group. HOPG substrate with oriented LC was prepared according to the method explained in section 3.1.2.2 and 3.1.2.3. A saturated solution of pure LC and C40 (1:10) was prepared and a droplet of this mixture was applied on the aligned LC sample. This sample was placed into the heating oven at 36 °C for 5 minutes with air circulation. The sample was then removed from the heating oven and cooled to room temperature (25 °C).

However, no *n*-alkane deposition was observed on the sample using optical microscopy. The details of these results are shown in Chapter 4. Thus, it was decided to adopt an alternative deposition method for growing *n*-alkane thin films.

### 3.1.2.5 Preparation of C40 Thin Films by PVD

A solution casting method was not successful for displacing the LC film during the *n*-alkane deposition, physical vacuum evaporator (PVD) was used to deposit the C40 alkane layers by epitaxy on the oriented LC thin film on HOPG. This instrument was described in Chapter 2.

The PVD process was used to deposit a thin film of *n*-alkane on the samples as shown in the Figure 3.5. Different substrates, with diluted or non-diluted LC were used or with the use or absence of a magnetic field at different temperature range (25 °C - 50 °C), were studied.

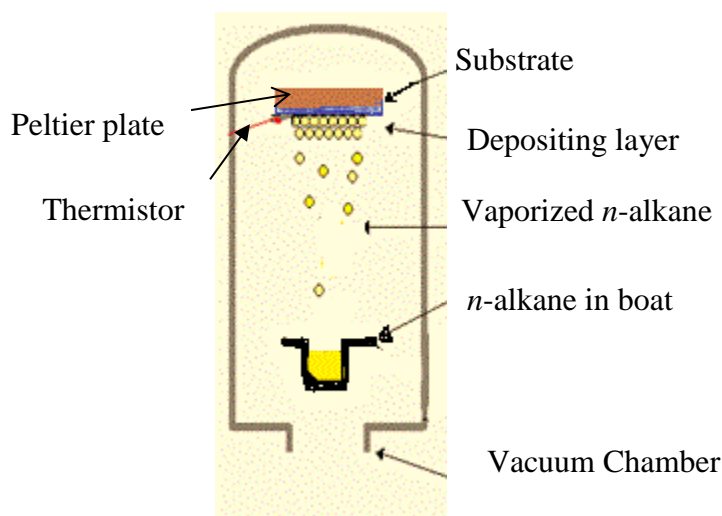


**Figure 3.5:** Process of thin film formation during the physical vapour deposition (PVD).

### 3.1.3 Characterization of *n*-Alkane Films

The morphologies of all the samples were investigated using a Nikon Eclipse ME600 optical microscope.

## **3.2 Orientation Control by Electric Field Alignment**

### **3.2.1 Experimental Approach**

A new experimental approach was developed to align LC sample with an electric field. In this new method NaCl(001) was selected as a non-conducting substrate. Thin films of LC were grown by placing a 1 $\mu$ L drop from a diluted LC crystal solution on the NaCl(001) surface. An electric field was then applied to the sample (NaCl+LC) by a specially designed electrode. Subsequently, a thin film of C40 was deposited by PVD on the top of the aligned sacrificial LC template. The detailed procedure of electric field alignment is already explained in Chapter 2. The samples were examined by optical microscope.

### **3.2.2 Sample Preparation for Electric Field Alignment**

#### **3.2.2.1 Substrate Selection**

During this experiment a non-conducting substrate was required to maintain a potential difference, so a NaCl(001) substrate was selected for LC orientation and for subsequent C40 deposition. Single crystals of NaCl were cleaved with a razor blade. A smooth surface was not possible, and the presence of kinks and ledges is expected to initiate the film nucleation process.<sup>60</sup>

#### **3.2.2.2 LC Film Preparation**

A drop (100 - 150 $\mu$ L) of LC diluted with ethanol (1:200) was placed on the freshly cleaved NaCl crystal with a micro syringe at room temperature. The LC was spread on the substrate surface and it made thin films on the substrate.

### **3.2.2.3 Application of Electric Field**

A thin film of the LC on NaCl(001) substrate was deposited and the sample was mounted on a specially designed Si<sub>3</sub>N<sub>4</sub> holder having gold electrodes. Both the gold electrodes were 1 mm apart with each other. An electric field of 20 V/mm was supplied to the sample for 2 minutes.

### **3.2.2.4 C40 Deposition**

PVD was used to deposit C40 on the oriented LC after electric field alignment. The procedure for growing thin films by PVD is already described in Chapter 2.

### **3.2.3 Characterization of *n*-Alkane Films**

Different sample morphologies were investigated using the Nikon Eclipse ME600 polarized optical microscope with bright field illumination at different lens magnifications.

## CHAPTER 4

### RESULTS AND DISCUSSION

This Chapter will present a detailed discussion and interpretation of the results for magnetic and electric field alignment methods.

#### 4.1 LC Film Preparation on HOPG

The first part of this research project was to reproduce the results obtained by the Patrick group for highly oriented *n*-alkane thin films using a magnetically oriented LC film as a template. HOPG was used as a substrate both in the form of a freshly cleaved HOPG surface and the HOPG flakes on a silicon surface. Initially, a small quantity of pure LC (a viscous gel at room temperature) was applied to the HOPG surface, but the gel-like material did not spread on the HOPG surface. A rectangular (1 x 1 inch) glass cover slip was used to distribute the gel-like LC layer on both regular HOPG surface and Kish graphite on the Si wafer substrate sample. Both samples were also heated to 100 °C. The LC gel did spread into a thinner film on both graphite surfaces.

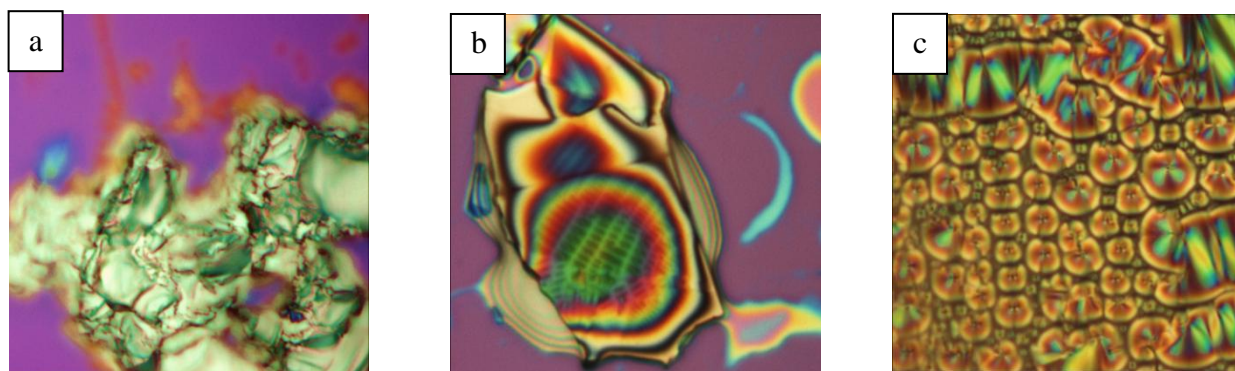


**Figure 4.1:** Polarized optical microscope images of the samples prepared by depositing (a) LC gel on Kish graphite on the silicon wafer sample at room temperature. (b) LC on Kish graphite on the silicon wafer after heating and spreading the LC gel with a glass coverslip. (c) LC on HOPG after heating and distributing by glass coverslip at 100X objective lens magnification and bright field illumination.



Figure 4.1(a) presents the LC on Kish graphite on the Si wafer substrate. The LC appears like a thick gel. In 4.1(b) and 4.2(c) the LC spread homogenously after heating and spreading the film with a glass cover slip. In 4.1(b), the LC is seen on the small flake of Kish graphite in the centre of the image.

After spreading the LC film, a solution casting method was applied for the deposition of C40 on the LC on HOPG substrate, as discussed in section 3.1.2.4. The sample was examined by polarized optical microscope and the sample showed only the presence of LC (characteristic birefringence) after deposition. No C40 deposition was observed by the optical microscopy as characterized by the absence of characteristic *n*-alkane 6-fold symmetry or oriented bars. The sample appeared to be same before and after the C40 deposition. It was hypothesized that excess LC was obscuring the *n*-alkane features. The excess LC was washed with ethanol. No C40 deposition was observed after washing the sample with ethanol.

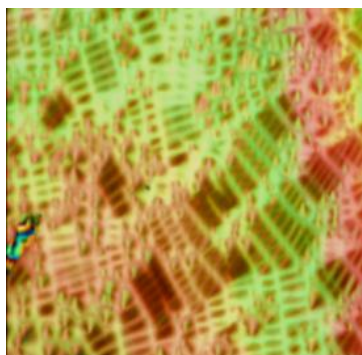


**Figure 4.2:** Polarized optical microscope image of a sample prepared by depositing C40 on oriented LC on HOPG by solution deposition method at 100X objective lens magnification and bright field illumination.

Figure 4.2 shows only the presence of LC on the graphite substrate after the C40 deposition. The above image is identical with Figure 4.1(c) which presents a LC film on the graphite surface. No *n*-alkane deposition was observed on the sample. Thus, it was decided to adopt an alternative

deposition method, so, physical vapor deposition was adopted for the epitaxially grown *n*-alkane thin films.

The samples were prepared by depositing a pure LC film on HOPG substrate and the LC films were oriented with a strong magnetic field, applied in the plane of the substrates. Subsequently, a film of C40 (50 nm) was deposited on top of the LC by PVD at 36 °C. The process of magnetic alignment and C40 deposition are explained in detail in Chapter 2 and 3. After the deposition, the samples were examined using polarized optical microscopy. Figure 4.3 presents the characteristic LC birefringence on the entire sample surface, indicating the presence of LC film. In this image, no characteristic C40 bars are observed. This is interpreted as evidence that the LC film was not displaced by the C40 deposition.



**Figure 4.3:** Polarized optical microscope image of a sample prepared by depositing C40 on LC on HOPG-ZYH substrate by PVD at 36 °C substrate temperature, at 100X objective lens magnification and bright field illumination.

During the early experiment by the Patrick group, it was observed that the 36 °C substrate temperature was the most suitable temperature for obtaining the preferred molecular orientation of the *n*-alkane in the LCI method.<sup>1</sup> Unfortunately, in this work characteristic bars of C40 were not observed on the HOPG substrate (Figure 4.3) at this temperature. Initially, it was assumed

that during the C40 deposition step, oriented LC molecules would be replaced by C40 molecules. As a thick LC film was still observed after C40 deposition, it was assumed that the LC layer was not dispersed. To aid the displacement of the LC gel, two approaches were examined: increase the substrate temperature during C40 deposition to aid the displacement of LC or dilute the LC with suitable solvent to form a thinner LC layer, which can more easily be replaced by C40 during the deposition process. When the C40 deposition temperature was raised to 50 °C the LC was displaced by a C40 film as observed by optical microscopy shown below in Figure 4.5. These results are described below.

### **Effect of LC on the *n*-Alkane Orientation at Different Deposition Temperatures**

This part of research work was done to determine to LC displacement temperature during C40 deposition. Pure LC was used to obtain these results.

### **Results and Discussion**

In the beginning of this research work, Kish graphite on a Si wafer substrate was used along with HOPG. Different morphologies of *n*-alkane were observed on graphite substrates when samples were prepared in the presence of LC film as compared to the samples which were prepared in the absence of LC at high substrate temperature. These samples were prepared without the magnetic alignment of LC, initially to determine the LC replacement process during C40 deposition.

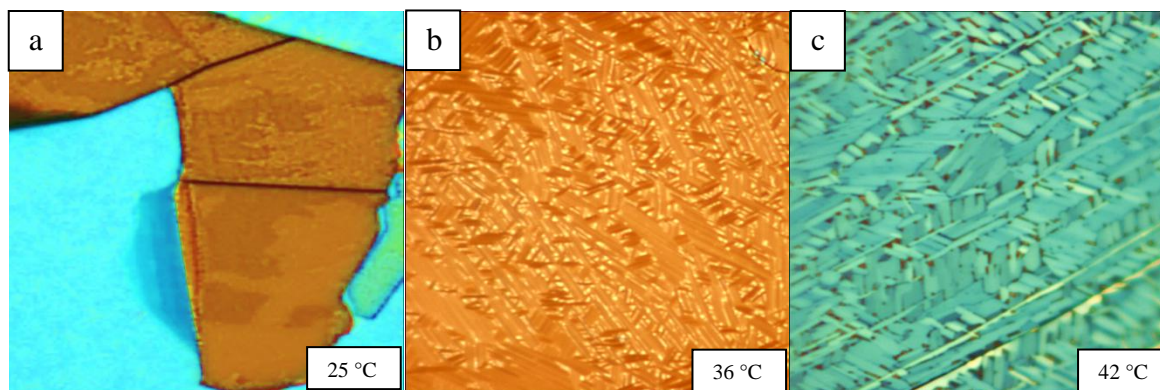


**Figure 4.4:** Polarized optical microscope images of the samples prepared by depositing C40 on (a) Kish graphite at 25 °C substrate temperature, (b) freshly cleaved HOPG at 36 °C substrate temperature and (c) freshly cleaved HOPG at 42 °C substrate temperature, at 100X objective lens magnification and bright field illumination.

Figure 4.4(a) shows a sample with C40 film that does not show bars with 6-fold symmetry. In Figure 4.4(b) and (c), the samples prepared at 36 °C and 42 °C substrate temperatures show *n*-alkane 6-fold symmetry on the HOPG surface. On the other hand, when these samples were prepared with a film of pure LC on the HOPG, the results indicate that the LC is not displaced after C40 deposition at 25 °C - 42 °C. The samples remain the same as shown in Figure 4.3.

The substrate temperature was gradually increased to 50 °C during C40 deposition. C40 bars with 6-fold symmetry are observed at 50 °C substrate temperature, which indicated that C40 molecules replaced the pure LC film. Figure 4.5 presents the *n*-alkane film morphology when deposited on HOPG at a high substrate temperature (50 °C). *N*-alkane pseudo rectangular structures are observed on graphite and the 6-fold symmetry was absent. On the contrary, when C40 is deposited on LC coated HOPG, the *n*-alkane deposit shows the 6-fold symmetry even at 50 °C (Figure 4.5b).

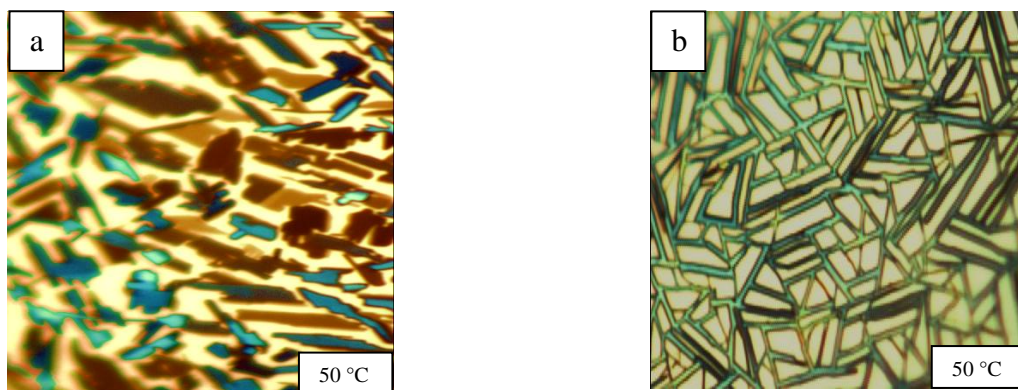


**Figure 4.5:** Polarized optical microscope images of the samples prepared by depositing C40 (a) in the absence of LC at 50 °C (b) in the presence of pure LC at 50 °C, at 100X objective lens magnification and bright field illumination.

At 36 °C and 42 °C substrate temperature, the pure LC was not replaced by the C40 molecules during the deposition process. At 50 °C, the LC film was displaced by C40 molecules and the *n*-alkane 6-fold symmetry was obtained.

To further explain the possible reasons for these structures, here is some description of the morphologies. Figure 4.4(a) presents light and dark film morphology with no *n*-alkane bars features at the 25 °C deposition temperature. This morphology shows the lateral orientation of *n*-alkane molecules on the substrate, because at low substrate temperature the molecules will be aligned parallel to the substrate.<sup>23</sup> When a C40 film is deposited on HOPG at 36 °C and 42 °C substrate temperatures (Figure 4.4(b) and (c) without LC), characteristic *n*-alkane 6-fold symmetry is seen. At 50 °C, *n*-alkane pseudo rectangular structures were observed.<sup>7</sup> However, in the presence of pure LC at the 50 °C deposition temperature the sample has exceptionally shown the *n*-alkane 6-fold symmetry, while other two samples prepared at 36 °C and 42 °C were still covered with the LC film (discussed earlier). In a previous study<sup>62</sup> the normal orientation of C40 molecules was observed at substrate temperature of 52 °C. In this work, the results at the 50 °C substrate temperature have only showed the parallel orientation of molecules, reflected by the 6-

fold symmetry. From these results, it was hypothesized that the LC molecules might help to increase the mobility of C40 and graphite surface during the deposition process, leading to stronger epitaxy. In future, work can be done to understand the interactions of *n*-alkane on graphite substrate in the presence of LC at elevated temperature, as the exact reasons for this behavior are not understood.

Although, the LC was replaced by C40 at 50 °C substrate temperature during the deposition process, but an alternative approach was used in order to reproduce the results for molecular orientation control at 36 °C substrate temperature during C40 deposition.

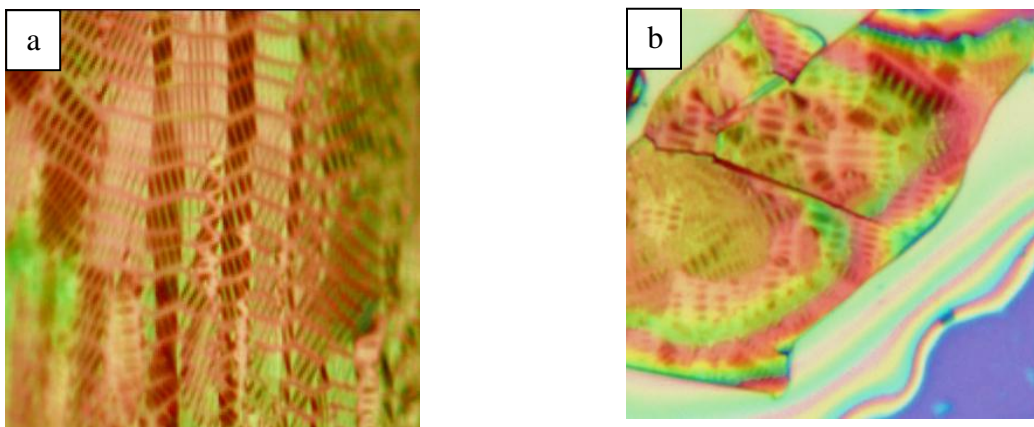
#### **LC Dilution Approach:**

In order to aid the displacement of LC by C40 deposition, solution casting of a thinner LC film was explored. In this approach, the LC was then diluted with different solvents (methanol, butanol, isopropanol and ethanol) and deposited on the HOPG in order to obtain a more uniform LC layer. Ethanol was ultimately selected for the dilution of LC because it gave a consistent spreading of the LC over the entire surface of both graphite substrates. Different ratios (8CB : ethanol) were prepared for the displacement of LC at 36 °C. It was later shown that the 1:50 ratio (8CB : ethanol) was the most suitable for the displacement of the LC by C40 during the deposition process at 36 °C substrate temperature.

#### **Results and Discussion:**

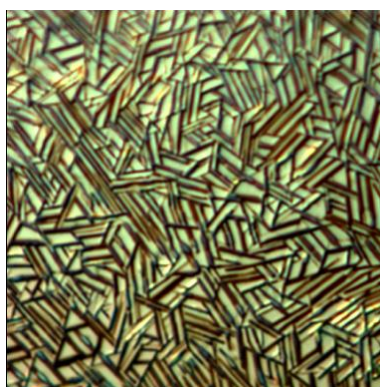
After finding the appropriate ratio of 8CB : ethanol, the experiment was resumed using both freshly cleaved HOPG and Kish graphite on the Si wafer substrates. Thin films of diluted LC on HOPG and Kish graphite on a Si wafer are shown below in Figure 4.6.





**Figure 4.6:** Polarized optical microscope images of the sample prepared by depositing LC on (a) HOPG-ZYH substrate (b) Kish graphite on the Si wafer substrate at room temperature, at 100X objective lens magnification and bright field illumination.

Figure 4.6(a) and 4.6(b) presents the polarized optical microscope images of the sample with diluted LC film on the two different substrates. The LC films appear similar on both substrates when observed by optical microscope. In both cases, the LC film is thin (not a thick gel) and is therefore expected to be replaced by C40 during the deposition. Subsequent observations have shown that these LC thin films were suitable for use as a sacrificial template.



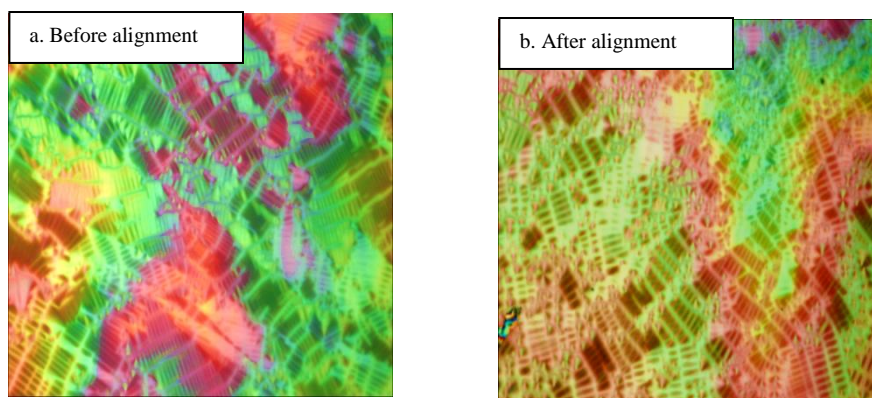
**Figure 4.7:** Polarized optical microscope image of a sample prepared by depositing C40 thin film on diluted LC with no magnetic field alignment on HOPG, at 36 °C substrate temperature, at 100X objective lens magnification and bright field illumination.

Figure 4.7 shows the effectiveness of the LC dilution approach which is demonstrated by its ability to be displaced by C40 deposition. Typical 6-fold symmetry<sup>7</sup> of an *n*-alkane film was

obtained, when C40 film was deposited on the diluted LC on HOPG substrate in the absence of magnetically aligned LC at 36 °C substrate temperature. This result proved that 1:50 (8CB:ethanol) was the most appropriate ratio for further experiments because all the LC was displaced by C40 indicated by polarized optical microscopy and *n*-alkane epitaxy resulted on HOPG substrate. This symmetry is responsible for trigonal pattern that can be observed by the *n*-alkane molecules in which the deposited crystallites are 60° to each other.<sup>20</sup>

#### 4.2 Effect of Magnetic Strength on the Orientation of *n*-Alkane Films

After determining the suitable LC dilution ratio, samples were prepared according to the methods discussed in Chapter 3. Diluted LC film was deposited on HOPG substrate and LC samples were aligned within the magnetic strength of 0.2 T – 2.3 T.



**Figure 4.8:** Polarized optical microscope image of a sample prepared by diluted 8CB thin film on HOPG substrate (a) before and (b) after alignment in a magnetic field at 100X objective lens magnification and bright field illumination.

After applying the different magnetic field strengths to LC samples, the LC film appears to be identical before and after the magnetic field alignment in all the samples. From Figure 4.8 (b) it was assumed that only the LC monolayer directly attached to the HOPG interface was oriented with the magnetic field and remains oriented afterwards. It was assumed that the oriented monolayer on the graphite interface can retain its induced alignment, while the bulk film can



relax and therefore the LC film can appear to be identical. Later, during the C40 deposition step, the orientation of LC monolayer was proved as shown below.

#### 4.2.1 Effect of Magnetic Field strength between 0.2 T - 2.0 T

The following results were obtained after C40 deposition on LC at 36 °C substrate temperature, when the LC was initially oriented within a magnetic field range of up to 1.0 T. The Bruker EPR magnets were used to orient the LC film.

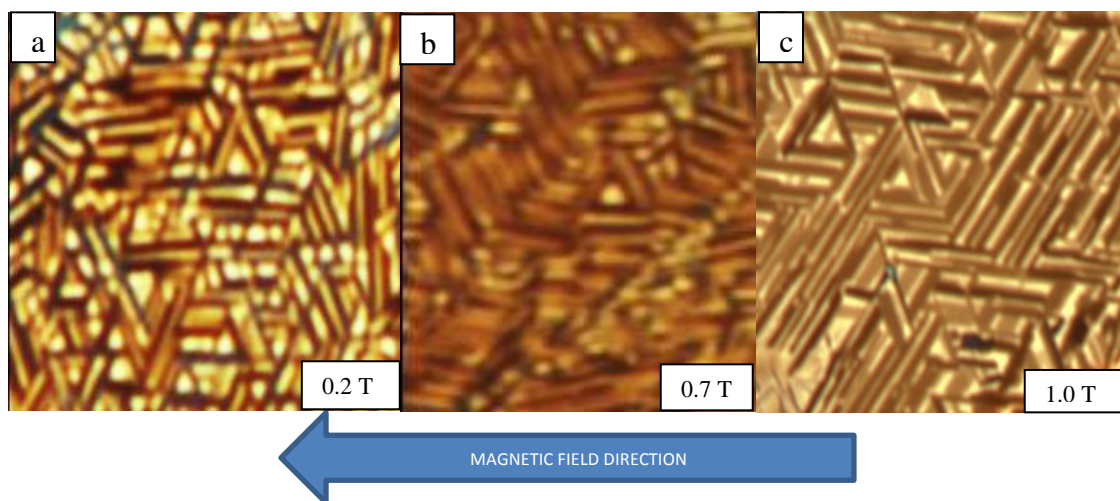


**Figure 4.9:** Polarized optical microscope images (magnified) of the samples prepared by depositing C40 on HOPG substrate at 36 °C, on top of diluted LC in the presence of different magnetic field strengths of (a) 0.2 T, (b) 0.7 T and (c) 1.0 T respectively at 100X objective lens and bright field illumination. The arrow sign is indicating the direction of magnetic field.

Figure 4.9 presents the polarized optical microscope images of the C40 deposition on a LC on HOPG where the LC is aligned with a magnetic field of 0.2 T - 1.0 T. It is observed that although a magnetic field of 0.2 T - 1.0 T was applied but all the samples still show the 6-fold symmetry. This 6-fold symmetry presumably indicates that the LC thin film was not aligned by the magnetic field, or did not act as a template. The samples prepared without the magnetic field and with the magnetic strength of 1.0 T show the same results as seen in Figure 4.7 and 4.9.

The same results were obtained with the Kish graphite on the Si wafer substrate, as shown in Figure 4.10. All the samples showed the 6-fold symmetry of *n*-alkane film on graphite which presents the absence of magnetic alignment of the LC film.

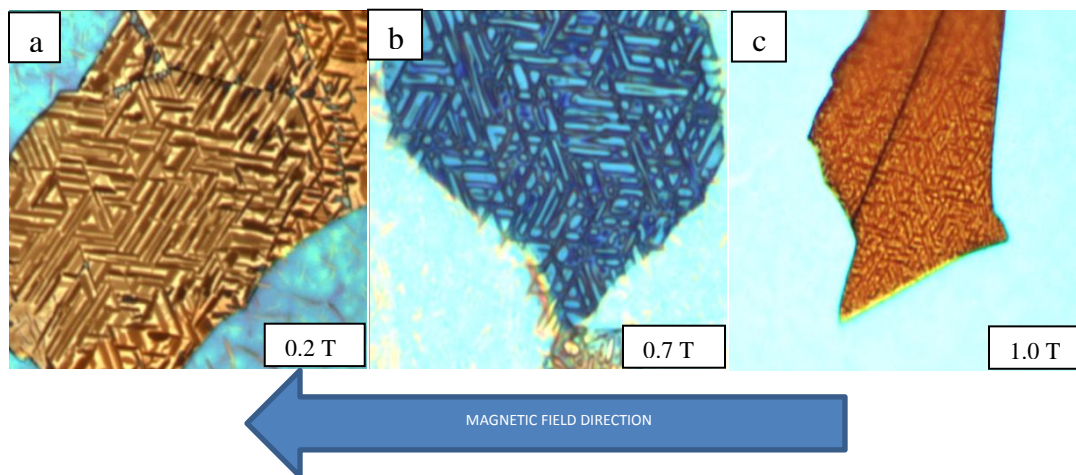


**Figure 4.10:** Polarized optical microscope images of C40 deposition on Kish graphite on the Si wafer substrate on top of diluted LC in the presence of different magnetic field strengths of (a) 0.2 T, (b) 0.7 T at 100X and (c) 1.0 T at 50X objective lens magnifications and bright field illumination.

It was hypothesized that the EPR Bruker magnets with magnetic strength of 1.0 T (10 KGauss) were not strong enough to orient the LC film at the HOPG - LC interface. A magnetic field was applied to orient the LC molecules so that it can control the *n*-alkane orientation by acting as a sacrificial template, but no orientational control in C40 thin film was observed. So, it was decided to work with stronger magnets. The Danfysik magnetic system from the magnet mapping lab (CLS), has a magnetic field strength of up to 3.0 T. Only the HOPG-ZYH substrate was used for this study, as the same results were also observed above for graphite on the Si wafer. A magnetic field of up to 2.0 T was applied to the diluted LC on HOPG in the plane of the sample surface. Subsequently, C40 was deposited by PVD. After the C40 deposition samples were observed under the optical microscope as shown in Figure 4.11.

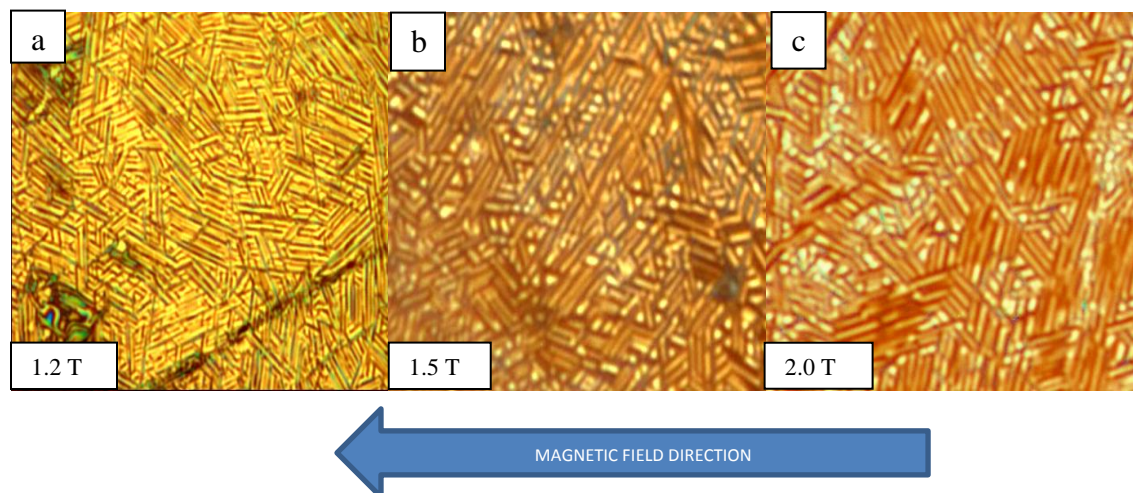


**Figure 4.11:** Polarized optical microscope images of the samples prepared by depositing C40 by PVD on HOPG at 36 °C substrate temperature on magnetically aligned diluted LC at different magnetic field strengths of (a) 1.2 T, (b) 1.5 T and (c) 2.0 T at 100X objective lens magnification and bright field illumination.

Even at 1.2 T and 1.5 T, the samples showed the 6-fold symmetry of *n*-alkane. However, at 2.0 T, some small structural changes in the 6-fold symmetry were observed. Some unidirectional bars were observed but only in a small area of the sample which indicated that some of the LC might orient so that these unidirectional bars were observed. It was assumed that by increasing the magnetic field strength could result the more orientation of LC film.

#### 4.2.2 Effect of Magnetic Field Strength between 2.0 T - 2.3 T

It was decided to continue the work with a stronger magnetic field, but the heating cell needed to be redesigned. A new heating cell was designed to reduce the distance between the magnetic poles. A magnetic strength of maximum 2.33 T could then be reached.



A LC film was oriented with the higher magnetic field strength of 2.3 T using a new heating cell. Afterward, C40 was deposited by PVD at 36 °C. The following results were obtained when samples were prepared with the high magnetic field strength.

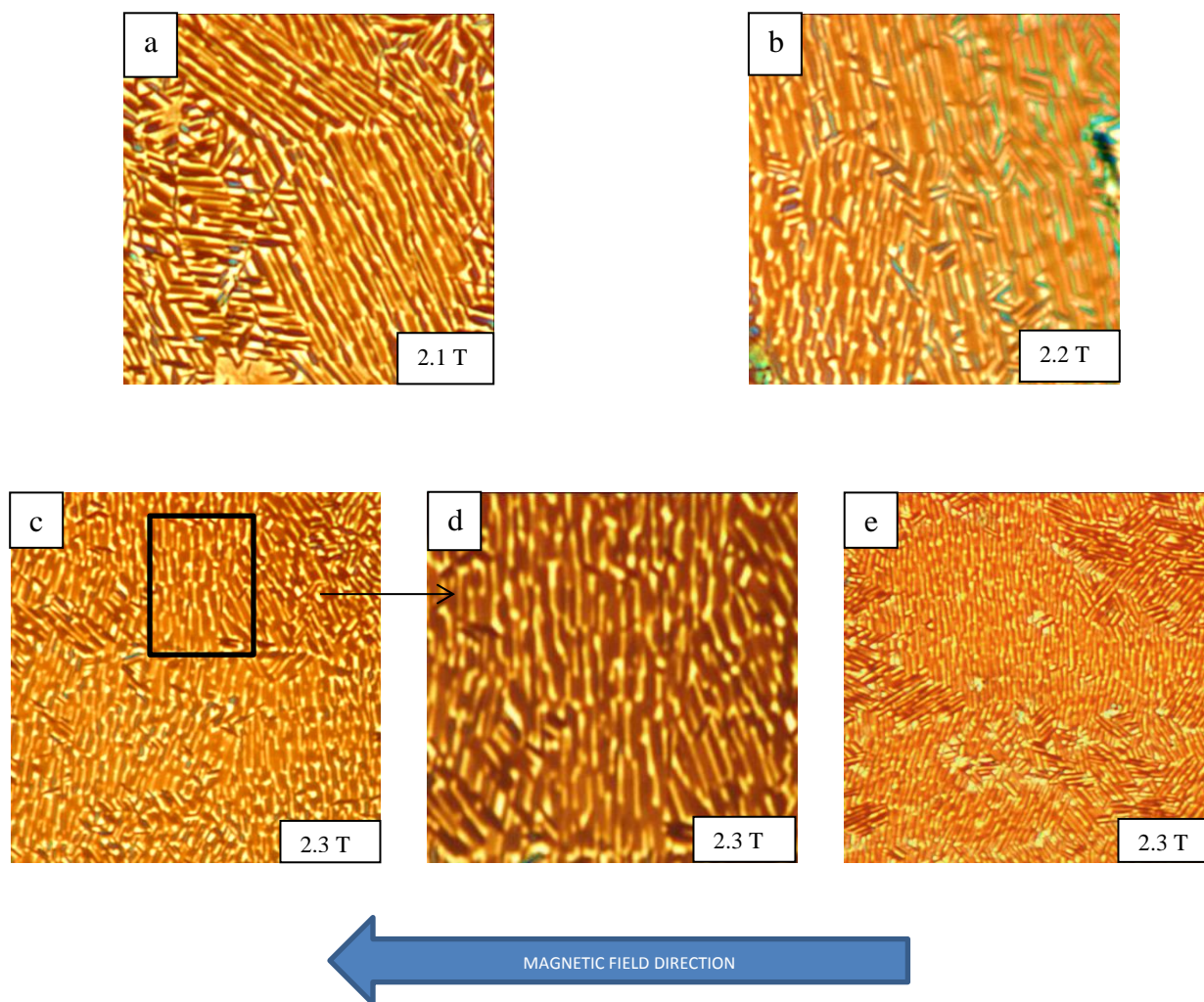


**Figure 4.12:** Polarized optical microscope images of the samples prepared by depositing C40 thin film on dilute LC on HOPG at 36 °C substrate temperature, after applying a magnetic field of (a) 2.1 T, (b) 2.2 T (c) 2.3 T and (d) magnified image after applying a magnetic field of 2.3 T at 100X objective lens magnification (e) 2.3 T at 50X objective lens magnification and bright field illumination.

Figure 4.12 (a) and (b) shows the C40 deposition on the oriented LC film when a magnetic field of 2.3 T was applied. Some parts of the sample showed the presence of vertical *n*-alkane bars, which were perpendicular to the applied magnetic field. The typical 6-fold symmetry of *n*-alkane

was absent or broken in the samples, in which the LC was oriented in the strong magnetic field. Above pictures shows that even with a small change in the magnetic field (above 2.1 T) strength the *n*-alkane bars changes the orientation prominently. When a magnetic field of 2.1 T was applied to the sample, the orientation of *n*-alkane bars was not perpendicular to the magnetic field as shown in Figure 4.12(a), while almost perpendicular *n*-alkane bars were observed at 2.2 T, or seen in Figure 4.12(b). However, perpendicular *n*-alkane bars were observed when a magnetic field of 2.3 T was applied. This indicated the presence of oriented C40 thin film by the sacrificial template act of the oriented LC.

Following Figure 4.13 presents the process of LC alignment, C40 deposition and the LC displacement by C40 based upon the concept of LCI.<sup>1</sup> An oriented *n*-alkane film can be obtained by this technique if the magnetic field is strong enough.

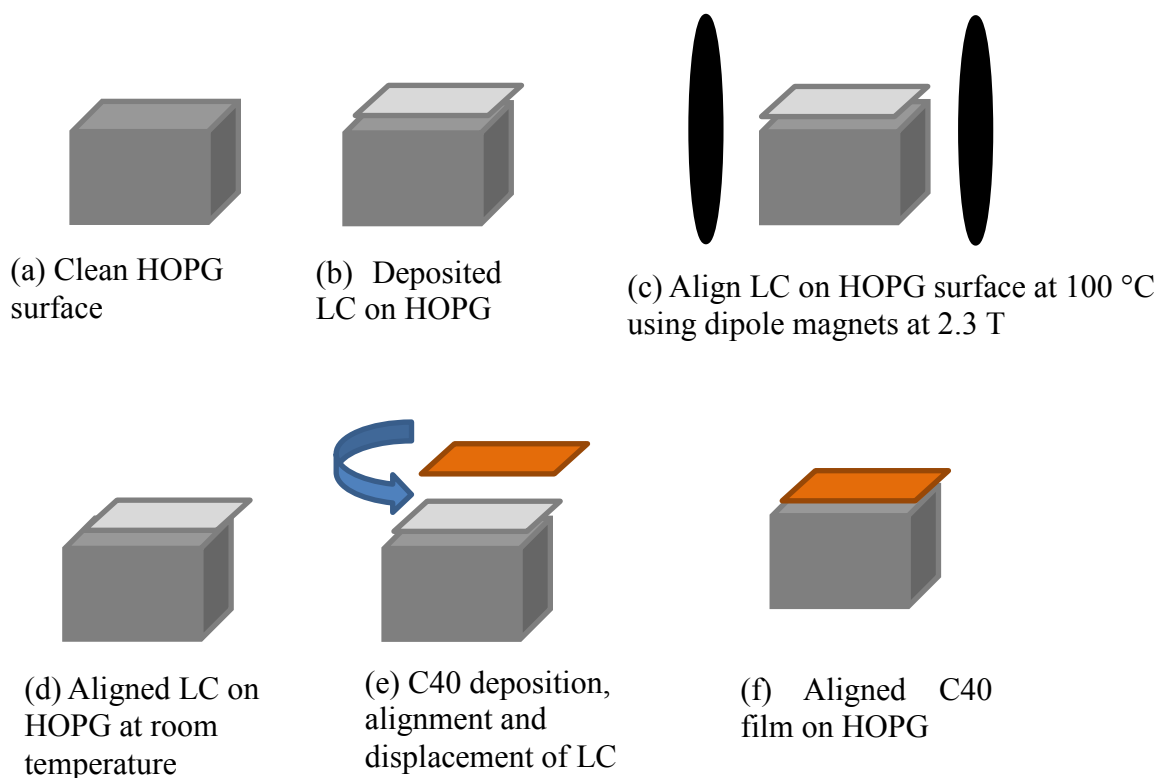


**Figure 4.13:** Step-by-step process for obtaining oriented C40 film using the LCI method.<sup>1</sup>

### 4.3 Discussion

During this study, the sacrificial template behavior of a magnetically aligned LC was studied for controlling the orientation of C40 molecules. The LC (4-octyl-4-cyanobiphenyl) is a viscous compound at room temperature. Previous studies have shown that it has an ability to form an ordered monolayer on graphite through epitaxial growth.<sup>61</sup> In this work, the orientation of the LC was controlled (predominantly on LC - HOPG interface) by using a strong magnetic field of 2.3 T, which was confirmed after C40 deposition.

According to Hickman *et al.*<sup>1</sup> the magnetic field strength of a few Tesla is enough to orient the LC molecules. In their work they used a magnetic field of 1.2 T for the orientation control experiment. Figure 4.9, 4.10 and 4.11 represent no orientation control in C40 thin films even when a magnetic field of up to 2.0 T was applied. All the samples showed only the characteristic 6-fold symmetry of *n*-alkane molecules after deposition on both kinds of graphite substrates. These samples were prepared in the magnetic field oriented in the sample plane. A hypothesis was developed after the experimental results when no orientation control was observed. According to this hypothesis, the magnetic field was not strong enough to orient the LC molecules on the graphite surface. It was expected that a magnetically oriented monolayer of LC on the HOPG surface would lead the oriented *n*-alkane film formation. However, all the samples showed only 6-fold symmetry of *n*-alkane with an optical microscope, which reflects unoriented epitaxy on the HOPG surface. However, the samples which were prepared with the magnetic field strength of 2.1 T, 2.2 T and 2.3 T showed the broken 6-fold symmetry after the C40 deposition. The vertical bars of *n*-alkane molecules were observed, which shows magnetic orientation control. Instead of characteristic *n*-alkane 6-fold symmetry, unidirectional oriented bars were observed. Thus, orientation of *n*-alkane molecules was controlled by magnetically oriented 8CB (LC), which acts as a sacrificial template.

It is evident from the Figure 4.14 that the *n*-alkane bars are perpendicular to the magnetic field and in each bar the *n*-alkane molecules are oriented parallel to each other.

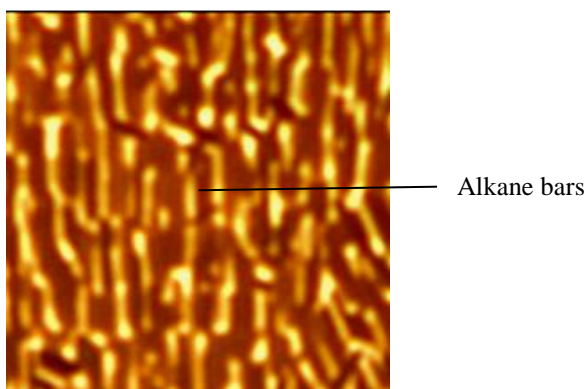


**Figure 4.14:** Polarized optical microscopic image (magnified) of a sample prepared by depositing C40 having vertically oriented *n*-alkane bars on HOPG substrate at 36 °C substrate temperature at 100X objective lens magnification and bright field illumination.

Fu *et al.*<sup>23</sup> proposed a model for the preferential side-by-side growth of C36 molecules in bars on NaCl(001) crystal. This model is also helpful to explain the C40 growth on the HOPG substrate. According to this model, *n*-alkane molecules have stronger inter chain (head-to-head) interactions as compared to head-to-tail interactions in a bar.<sup>23</sup> So, it was hypothesized that *n*-alkane molecules were oriented perpendicular to the individual bar but every molecule oriented parallel to individual molecule which was proved by X-ray microscopy.<sup>23</sup>

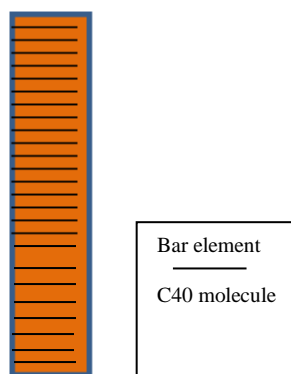


**Figure 4.15:** Parallel (side-by-side) position of C40 molecules in a bar like structures, on the basis of the model proposed by J. Fu *et al.*<sup>23</sup>

Figure 4.15 presents an individual *n*-alkane bar, and the individual *n*-alkane molecules in the bar, which are parallel to each other indicates that during the magnetic field alignment of LC, the LC molecules were oriented parallel to the magnetic field, and subsequently aligned the *n*-alkane.

The results presented in this research work can be best explained with the model proposed earlier by Patrick group.<sup>1</sup> Based on this model, it was hypothesized that during the C40 deposition on the oriented LC (8CB) film, the *n*-alkane molecules diffused through the oriented LC. Then two 8CB molecules which were initially oriented parallel to the magnetic field were replaced by C40. This replacement process was repeated on the entire surface of the graphite-LC interface, then at appropriate deposition rate and temperature a layer of C40 (50 nm) was grown. During the C40 deposition the substrate temperature was maintained at 36 °C, and also it is the temperature of the nematic phase of LC in which molecules have orientation order with mobility. During epitaxial growth the guest molecular chains copy the host crystal lattice orientation. Finally, oriented C40 films were obtained and observed using the optical microscope. Molecular orientation at the nanoscale cannot be observed by optical microscopy, however, *n*-alkane bars symmetry can be observed at the microscale.

### **Comparison of Patrick Results:**

From the above results, (Figure 4.12) orientation control by using LC as a sacrificial template was reproduced. During the experiment,<sup>1</sup> they used a magnetic field of 1.2 T for orienting a LC film which later acted as a sacrificial template for obtaining an oriented *n*-alkane film. In this thesis work orientation control was not observed in *n*-alkane samples when LC was oriented at 1.2 T. Similarly, up to 2.0 T no orientation control was observed. A stronger magnetic field of 2.3 T was needed to orient the LC film. During this research work a solution of diluted LC was



used because pure LC was appeared as a gel-like layer on the substrate and during the deposition process, this LC was not replaced by C40. In the previous work, the orientation control of an in the *n*-alkane monolayer was studied but in this work the orientation control in the epitaxially grown *n*-alkane multilayer thin film was observed.

#### **4.4 *N*-Alkane Film Preparation on Electrically Aligned LC**

A new method was developed to extend and modify the previous method of magnetically aligned LC orientation by using an electric field instead. An electric field was applied to orient the LC on a NaCl(001) substrate between gold electrodes on Si<sub>3</sub>N<sub>4</sub> window. The LC dipole moment tends to orient along the direction of electric field.<sup>45</sup> Later C40 was deposited by PVD. The results obtained after this experiment are explained in detail in the following section

##### **4.4.1 *N*-Alkane Film Preparation on Different Samples**

A freshly cleaved NaCl(001) substrate was used for the electric field alignment of the LC. In the last few decades a lot of work was done with the alkali halide substrates as discussed in Chapter On the NaCl(001) substrate, *n*-alkane molecules usually form structures with 4-fold symmetry<sup>23</sup> when grown epitaxially. A very dilute LC solution 1:200 (LC : ethanol) was prepared because the previous diluted LC solution 1:50 (LC : ethanol) was not able to make very thin film. The appearance of the LC on the NaCl substrate was almost transparent as shown in the Figure 4.16.

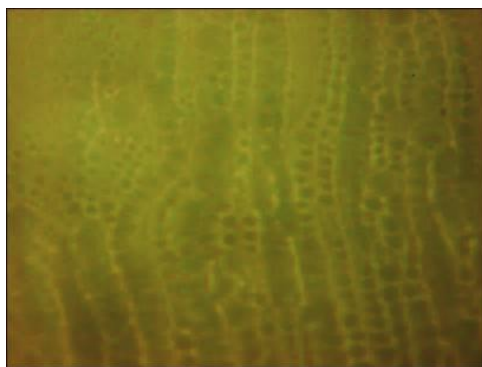


**Figure 4.16:** Polarized optical microscope image a sample having a LC thin film on freshly cleaved NaCl substrate at 100X objective lens magnification and dark field illumination.

Several samples were prepared for comparison:

- (a) A sample was prepared by depositing C40 on NaCl(001) at 36 °C substrate temperature.
- (b) Other sample was prepared by depositing C40 on LC film on NaCl(001) at 36 °C substrate temperature. No electric field was used to orient the LC film.
- (c) Another sample was prepared by depositing C40 on LC film on NaCl(001) at 36 °C substrate temperature. A 20 V/mm electric field was used to orient the LC film before C40 deposition.

The characteristic 4-fold symmetry of epitaxially grown *n*-alkane was observed on NaCl substrate as shown in Figure 4.17(a). Figure 4.17(b) presents the 4-fold symmetry of *n*-alkane in the presence of a thin LC film without electric field alignment, on the NaCl(001) substrate.

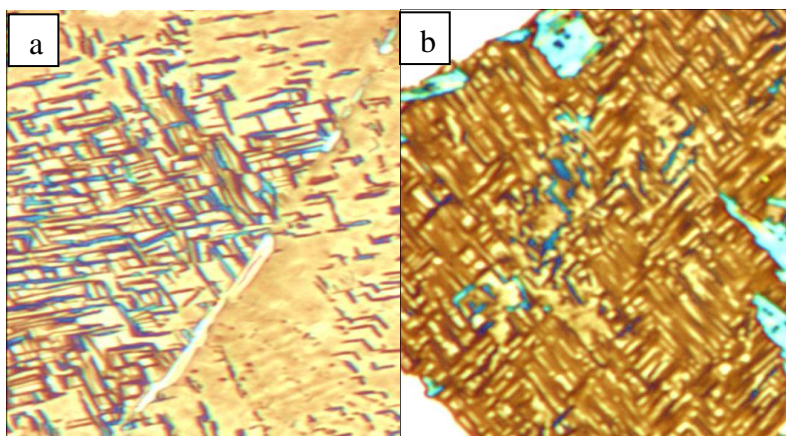


**Figure 4.17:** Polarized optical microscope images of the samples prepared by depositing C40 on (a) NaCl(001) substrate at 36 °C substrate temperature (b) NaCl(001) substrate having diluted LC at 36 °C substrate temperature without applying electric field, at 100X objective lens magnification and bright field illumination.

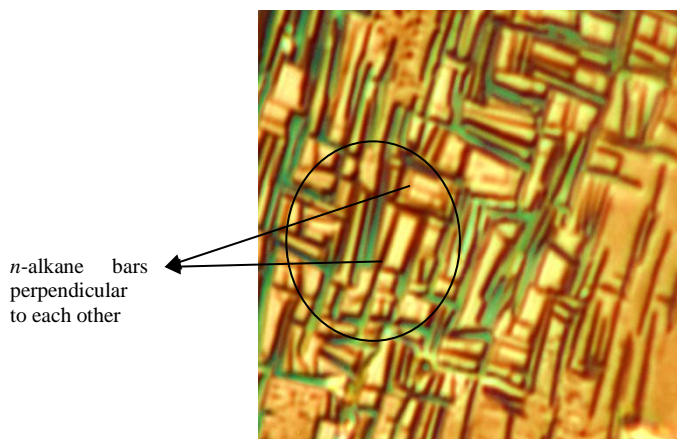


**Figure 4.18:** Polarized optical microscope image (magnified) of a sample prepared by depositing C40 thin films on NaCl substrate having bars at 90° to each other at 100X objective lens magnification and bright field illumination.

Figure 4.18 shows the *n*-alkane 4-fold symmetry having alkane bars at 90° to each other on NaCl substrate. Thus, 4-fold symmetry of *n*-alkane was obtained even in the presence of LC. Now, to see the effect of electric field on the orientation of LC molecules, a sample was prepared by applying an electric field (20 V/mm) on a NaCl/LC substrate, followed by C40 deposition at 36

°C substrate temperature. Figure 4.19 presents three different kinds of alkane morphologies on NaCl substrate when sample was prepared in the presence of electrically oriented LC.

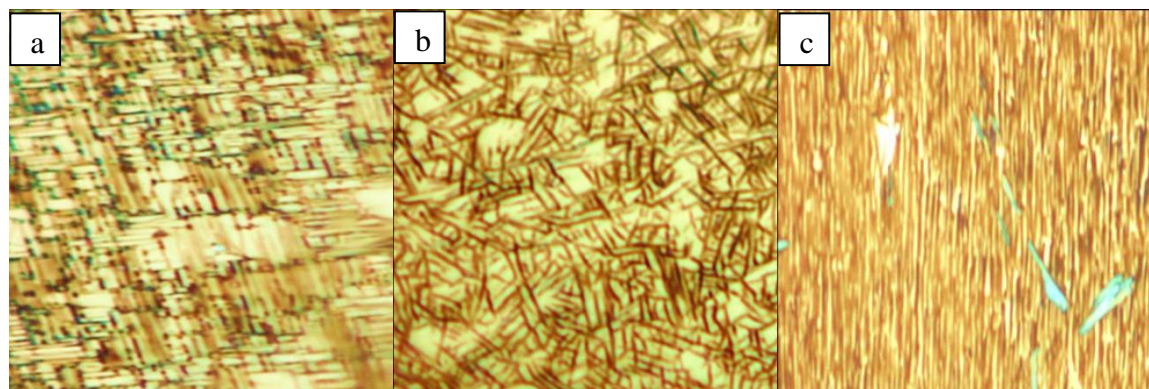


**Figure 4.19:** Polarized optical microscope images of a sample prepared by depositing *n*-alkane film on electrically oriented LC on NaCl(001) substrate at 36 °C substrate temperature, having (a) 4-fold symmetry (b) broken 4-fold symmetry (c) vertically oriented *n*-alkane bars at 100X objective lens magnification and bright field illumination.

Figure 4.19 presents three different *n*-alkane morphologies (a) 4-fold symmetry (b) randomly oriented bars or broken 4-fold symmetry and (c) highly oriented uni-direction *n*-alkane bars on a NaCl substrate at 36 °C in the presence of oriented LC.

Figure 4.20 shows the presence of three different morphologies on the same sample. The border among these three morphologies is also shown. The presence of unidirectional bars, even at low voltage was the success of the experiment.

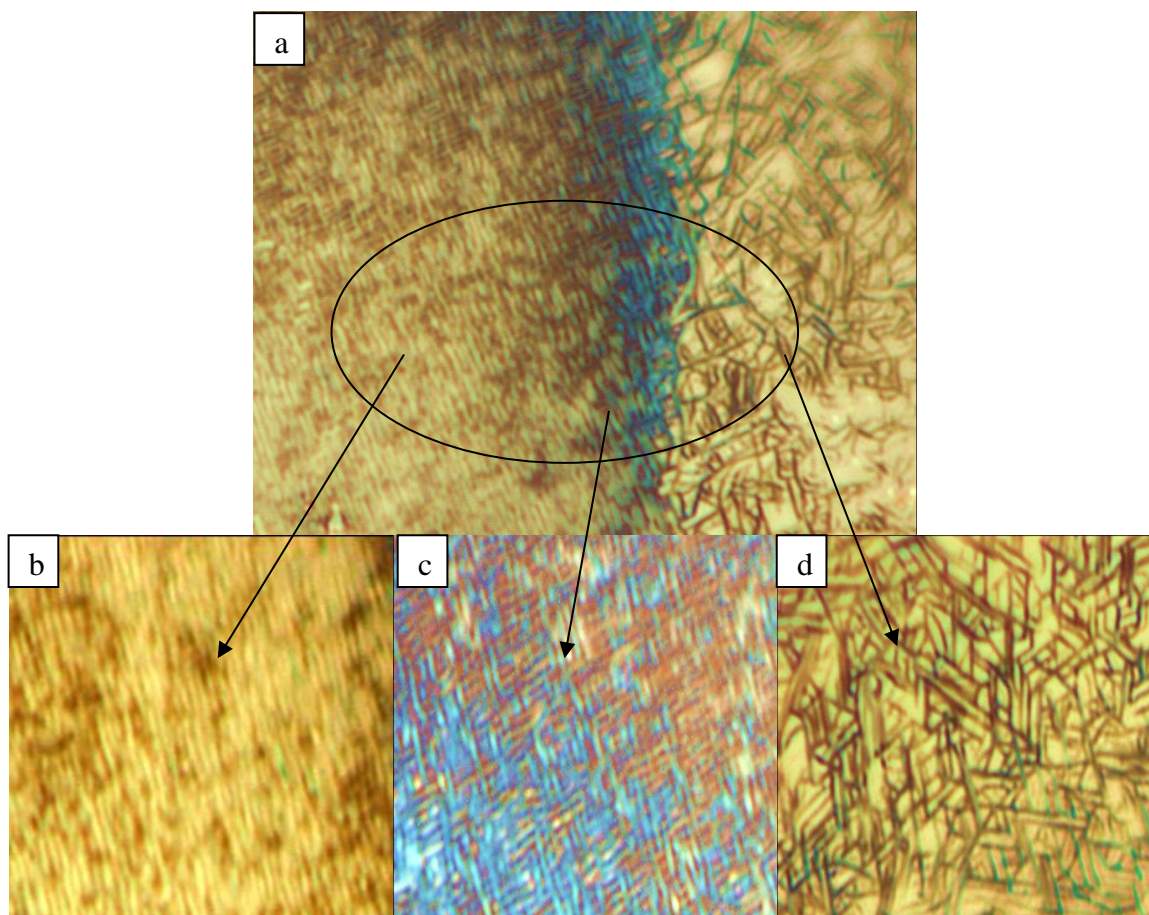


**Figure 4.20:** Polarized optical microscope images of a sample prepared by depositing C40 film on NaCl (001), with electrically oriented LC on NaCl(001) substrate at 36 °C substrate temperature having (a) all three different morphologies of C40 orientation (b) vertically oriented *n*-alkane bars (c) 4-fold symmetry (d) broken 4-fold symmetry at 100X objective lens magnification and bright field illumination.

#### 4.5 Discussion

From this newly developed method for molecular orientation control it was possible to obtain highly oriented (unidirectional bars) *n*-alkane films using an electric field at least in some area of the sample. In Figure 4.19(c) the highly ordered unidirectional *n*-alkane bars were obtained which represents the orientation control in epitaxially grown thin films. The LC (8CB) molecule has a permanent electric dipole. When an external electric field was applied to the LC, the molecule will tend to orient along the direction of the field and align parallel to this field. When C40



molecules were deposited on top of oriented LC molecules, the LC molecules will act as a sacrificial template and the C40 molecules diffused and replaced the oriented LC molecules based upon the idea of LCI.<sup>1</sup> The C40 molecules adopted the parallel orientation of aligned LC molecules which result unidirectional bars (Figure 4.19c). These bars are made up of *n*-alkane molecules positioned parallel to each other in the vertical bar as shown in Figure 4.15. Thus, over a large area highly oriented unidirectional bars were observed. Figure 4.20(b) and (c) shows two other *n*-alkane morphologies which were also obtained along with the unidirectional bars. *N*-alkane 4-fold symmetry was observed as shown in Figure 4.20(c), which is exactly the same as Figure 4.17(b), when a sample was prepared without any electric field on LC film on NaCl substrate. To understand the reason for these structural variations in Figure 4.20(d) two postulates were articulated. First, it might possible that initially the LC film has different thickness due to non-uniform flatness of the NaCl(001) substrate surface. Second, it might be possible that after the removal of electric field application, the orientation of LC molecules became randomized.

It was assumed that during the electric field alignment experiment the strength of the field was not strong enough to orient most of the LC film on NaCl substrate. It was decided to increase the electric field supply and reduce the time difference (approximately 1 hour) between the LC orientation step and the deposition process to minimize the exceptional results. A new voltage supply cell was designed for the *in situ* experiment. It was proposed to perform the LC alignment and C40 deposition simultaneously within the evaporator but due to contamination of the vacuum chamber it was not possible to proceed further with the experiment.

## 4.6 Experimental Challenges

In the orientation control experiment, many challenges were faced. Previous studies<sup>1</sup> have shown that HOPG is a suitable substrate for LC alignment. During the research, efforts were done to obtain another suitable substrate which could replace HOPG and to compare experimental results. HOPG is a thick substrate it was not suitable for investigation by Scanning Transmission X-ray Microscopy (STXM). Therefore, the preparation of an X-ray transparent substrate was tried for further study of molecular orientation. For example, thin layers of freshly cleaved Kish graphite were prepared. In initial experiments with Kish graphite and HOPG the same results were obtained. Still, it was difficult to prepare very thin substrates for STXM. A main focus of the magnetic field alignment experiment was to reproduce the results obtained by Patrick group, further work focused on HOPG and work with the Kish graphite substrate was abandoned.

To reproduce the results from the Patrick work for molecular orientation control, the same experimental procedure and chemicals were used as far as possible. Their studies had shown that 36 °C was the most suitable temperature for depositing C40 layer on oriented LC for maximum molecular orientation control. LC (8CB) is a very viscous compound and at room temperature it appeared as a gel when it was deposited on the graphite substrate. Although LC could be spread into a film by pressing it with a glass cover slip with applied heat, upon cooling it reformed as a thick layer. During the C40 deposition process on the thick LC gel, the LC film was not replaced by C40 at 36 °C substrate temperature, as expected.<sup>1</sup> The substrate temperature was increased gradually to 50 °C to promote LC displacement process. However, to be consistent with the literature, 36 °C substrate temperature was retained for the deposition process. It was assumed that the thickness of LC might be the reason for not obtaining the previous results. The idea of LC dilution was developed. After working with different ratios of 8CB : ethanol, a ratio 1:50

(8CB : ethanol) was selected to continue the experiment and when the experiment was conducted with diluted LC, the previous results were reproduced. The finding of appropriate dilution ratio was a challenge and it took a lot of time to optimize.

Previous results of the Patrick group have shown that a magnetic field of 1.2 T was enough to orient the pure LC film, presumably at the graphite-LC interface. During this experiment, it was not possible to obtain the same results using the magnetic strength of 1.2 T. It was one of the challenges to determine the required magnetic field to orient the diluted LC thin film. Initially EPR magnets were used from SSSC laboratory having a magnetic field of up to 1.0 T. When the LC was oriented within this range and then the C40 was deposited, no orientation order was observed. Therefore, it was decided to work with higher magnetic field strength and, hence, dipole magnets from the magnetic mapping lab at CLS were used. A magnetic strength of 2.3 T was used to obtain the molecular orientation control in epitaxially grown *n*-alkane films.

During the experiments the alignment of the LC within the magnetic field (or electric field) and the deposition of C40 were done in two separate steps. This created a suspicion that, perhaps, some of the LC randomized before the deposition. A new sample holder was designed to do the *in situ* experiment for the simultaneous LC electric field alignment and C40 deposition within the vacuum chamber, but due to LC contamination of the PVD chamber, this experiment was not possible.

During the *n*-alkane deposition process, the vacuum chamber was contaminated by the LC displacement as LC molecules became entrapped in the diffusion and rotary pump oil. These entrapped LC molecules contaminated other samples. Debugging these issues also took a lot of time.



## CHAPTER 5

### CONCLUSIONS

The main objective of this research work was to control the molecular orientation in the epitaxially grown *n*-alkane thin films. Two experimental approaches were adopted, the first goal of this project was to control the molecular orientation based upon an existing magnetic field alignment method<sup>1</sup> for the epitaxially grown *n*-alkane films. The second goal was to develop a new electric field alignment method for inducing a preferred molecular alignment in the growth of *n*-alkane thin films. This research work based upon the concept of LCI technique.<sup>1</sup> In the previous experiment by the Patrick group, a magnetic field of 1.2 T was used to orient a pure LC film and then *n*-alkane was deposited on the oriented LC film which acted as a sacrificial template<sup>1</sup> for orientation control of the *n*-alkane monolayers. In this work, the conditions for magnetic orientation of the LC film on graphite substrate were different and a stronger magnetic field of 2.3 T was used to orient a LC film and subsequently, a layer of C40 was deposited on top of the oriented diluted LC by physical vapour deposition (PVD). The samples were examined with the polarized optical microscopy.

Another new method was successfully developed by modifying the concept of LCI technique<sup>1</sup> by using an electric field for LC alignment. Electrodes (gold on Si<sub>3</sub>N<sub>4</sub>) were designed to hold the sample (LC on NaCl crystal) in an electric field of 20 V/mm for LC orientation. C40 films were then grown by PVD on the oriented LC. Unidirectional oriented bars were observed on some area of the NaCl(001) substrate, even at this low electric field. *N*-Alkane 4-fold and broken 4-fold symmetry was also observed within the same sample on the NaCl substrate. In brief, LC molecules were oriented by both the electric and magnetic field and during the deposition of *n*-

alkanes, these oriented LC molecules were replaced by C40 molecules and highly oriented *n*-alkane films were obtained.

To conclude, both methods could be used to obtain a preferable molecular orientation, by using the oriented LC to guide the growth of thin *n*-alkane films. However, in the future these methods can be further modified and refined either working with higher electric field strengths or by adopting alternative methods of *n*-alkane film deposition.

## CHAPTER 6

### Future Work

In the future, it is proposed to obtain highly oriented *n*-alkane films on the NaCl(001) substrate. The results in this work have shown the orientation control in the *n*-alkane films by using an oriented LC as a sacrificial template. Few research ideas have been proposed for higher orientation control in the *n*-alkane thin films for the next work. In the future work, it is proposed to use short chain *n*-alkane C36 (C<sub>36</sub>H<sub>74</sub>), along with C44 (C<sub>44</sub>H<sub>90</sub>), C50 (C<sub>50</sub>H<sub>102</sub>) and long chain *n*-alkane C60 (C<sub>60</sub>H<sub>122</sub>) molecules.

1. In the future, it is proposed to adopt solution casting method<sup>20</sup> for the epitaxial growth of *n*-alkane films, in order to avoid the LC contamination issue, which was faced during PVD. According to the this approach, the LC film will be oriented on a NaCl(001) substrate using a strong electric field. Then, the sample with oriented LC on NaCl substrate will be placed in *n*-alkane solution at a particular temperature. During the process the LC molecules will be displaced by *n*-alkane. Oriented *n*-alkane thin films will be obtained by solution deposition method (with suitable solvent system) by replacing the oriented LC film.
2. In the next work, it is also proposed to do the *in situ* *n*-alkane deposition process by solution casting method, simultaneously when the LC alignment (by electric field) will be done on the NaCl(001) substrate. This method might be helpful to displace the oriented LC by *n*-alkane in a short time and it might be useful to obtain the highly oriented *n*-alkane films. There are more chances of obtaining highly oriented *n*-alkanes because LC might not have time to randomize (as proposed during the electric field alignment process in Chapter 4).

## References

1. Hickman, S.; Hamilton, A.; Patrick, D. L., *J. Surf. Sci.* **2003**, 537, 113.
2. Royer, L. *Bull. Soc. Franc. Min.* **1928**, 51, 7.
3. Pashley, D.W. *Advance. Phys.* **1956**, 5, 173.
4. Ward, M. D. *Chem. Rev.* **2001**, 101, 1697.
5. Forrest. S. R. *Chem. Rev.* **1997**, 97, 1799.
6. Charig, J. M.; Joyce, B. A. *J. Electrochem. Soc.* **1962**, 109, 957.
7. Masnadi, M.; Urquhart , S. *Langmuir*, **2012**, 28, 12493.
8. Smith, L.D. *Thin Film Deposition Principles & Practice*; McGraw-Hill: U.S.A., **1995**.
9. Mobus, M.; Karl, N.; Kobayashi, T. *J. Cryst. Growth* **1992**, 116, 495.
10. Burrows, P. E.; Zhang, Y.; Haskal, E. I.; Forrest, S. R. *Appl. Phys. Lett.* **1992**, 61, 2417.
11. Kainuma, Y.; Uyede, R. *J. Phys. Soc. Jpn.* **1950**, 5, 199.
12. Suito, E. N.; Uyeda, R.; Ashida, M. *Nature*, **1962**, 194, 273.
13. Ueda. Y.; Ashida, M. *J. Electr. Microsp.* **1980**, 29, 38.
14. Wellinghoff, S.; Rybnikar, F.; Baer, E. *J. Macromol. Sci.* **1974**, 97, 1973.
15. Mauritz, K. A.; Baer, E.; Hopfinger, A. J. *J. Polym. Sci.* **1973**, 11, 2185.
16. Mauritz, K. A.; Baer, E.; Hopfinger, A. J. *J. Polym. Sci. Macromol Rev.* **1978**, 13, 1.
17. Hentschke, R.; Askadskaya, L. *J. Chem. Phys.* **1992**, 97, 6901.
18. Hosoi, Y.; Sakuri, Y.; Yamamoto, M.; Ishii, H.; Ouchi, Y.; Seki, K. *Surf. Sci.* **2002**, 515, 157.
19. Rabe, J. P.; Buchholz, S. *Science* **1991**, 23, 424.
20. Leunissen, E. M.; Graswinckel, W.S.; Enckevort, J. P. W.; Vlieg, E. *Cryst. Growth & Des.* **2004**, 4, 363.
21. Cincotti, S.; Rabe, J. P. *Appl. Phys. Lett.* **1993**, 62, 3531.

22. Shimizu, H.; Tanigaki, N.; Nakayama, K. *Jpn. J. Appl. Phys.* **1995**, 34, 701.
23. Fu, J.; Urquhart, S. G. *Langmuir* **2007**, 23, 2615.
24. Pashley, D. W. *Mater. Sci. Technol.* **1999**, 15, 2.
25. Forrest, S. R. *Chem. Rev.* **1997**, 97, 1799.
26. Kubono, A.; Okui, N. *Prog. Polym. Sci.* **1994**, 19, 389.
27. Tanka, K.; Okui, N.; Sakai, T.; *Thin Solid Films* **1991**, 196, 137.
28. Saito, Y.; Inaoka, K.; Kaito, C.; Okada, M.; *App. Surf. Sci.* **1988**, 33-34, 1298.
29. Kubono, A.; Akiyama, R.; *Mol. Cryst. Liq. Cryst.* **2001**, 378, 167.
30. Kubono, A.; Minagawa, Yuko.; Ito, T.; *J. Appl. Phys.* **2009**, 48, 0202111.
31. Dimitrakopoulos, C. D.; Mascaro, D. J. *IBM. J. Res. & Dev.* **2001**, 45, 11.
32. Shao, Y.; Yang, Y. *App Phys Lett.* **2005**, 86, 73510.
33. Wang, L.; Fine, D.; Dodabalapur, A. *App Phys Lett.* **2004**, 85, 6386.
34. Hooks, D. E.; Fritz, T.; Ward, M. D. *Adv. Mater.* **2001**, 13, 227.
35. Zhang, P. W.; Dorset, D. L. *J. Polym. Sci.* **1989**, 27, 1433.
36. Pereira, G. G.; Williams, D. R. M. *Macromol. Chem.* **1999**, 32, 8115.
37. Albrecht, T. T.; DeRouchey, J.; Russel, T. P.; Jaeger, H. M. *Macromolecules*, **2000**, 33, 3250.
38. Xiang, H.; Lin, Y.; Russel, T. P. *Macromolecules*, **2004**, 37, 5358.
39. Hatashi, K.; Kawato, S.; Fujii, T. H.; Matsushige, K. *Appl. Phys. Lett.* **1997**, 70, 1384.
40. Rudhardt, D.; Neives, A. F.; Link, D. R.; Weitz, D. A. *Appl. Phys. Lett.* **2003**, 82, 2610.
41. Kossyrev, P. A.; Yin, A.; Cloutier, S. G.; Cardimona, D. A.; Huang, D.; Alsing, P. M.; Xu, J. *M. Nano Lett.* **2005**, 10, 1978.
42. Neives, A. F.; Link, D. R.; Rudhardt, D.; Weitz, D. A. *Phys. Rev. Lett.* **2004**, 92, 105503.

43. Paineau, E.; Dozov, I.; Antova, K.; Imperor, M.; Michot J. L. *IOP Conf. Ser. Mater. Sci. Eng.* **2011**, *18*, 0620051.
44. Papadantonakis, M. K.; Brunschwig, S. B.; Lewis, S. N. *Langmuir*, **2008**, *24*, 857.
45. Collings, J. P. *Liquid Crystals*; Princeton University Press: U.S.A., 2002.
46. Madhusudana, V. N. *Current Science*, **2001**, *80*, 1018.
47. Lynch, D. M.; Patrick, L. D. *Nano Lett.* **2002**, *2*, 1197.
48. Mougous, J. D.; Brackley, A. D.; Foland, K.; Baker, R. T.; Patrick, D. L., *Phys. Rev. Lett.* **2000**, *84*, 2742.
49. Gislason, E. N.; Murphy, C.; Patrick L. D. *J. Phys. Chem. C* **2010**, *114*, 12659.
50. Chandrasekar, S. *Liquid Crystals* 2<sup>nd</sup> Edition; Cambridge University Press: U.K., **1992**.
51. Liquid crystal in external field, information page,  
<http://dept.kent.edu/spie/liquidcrystals/emfield1.html> (accessed June 28, 2012)
52. Ratna, B. R.; Shashidhar, R., *Mol. Cryst. Liq. Cryst.* **1977**, *42*, 113.
53. GMW Associates, Model 3474-140, 250 MM Electromagnet user manual, **2002**.
54. Nikon Eclipse ME 600P/600D, capraoptical.com.  
[http://www.capraoptical.com/products/nikon/High\\_Power\\_Microscopes/me600D600P.html](http://www.capraoptical.com/products/nikon/High_Power_Microscopes/me600D600P.html)  
 (accessed August 17, 2012)
55. Oblique Illumination, 2012. Olympusmicro.com.  
<http://www.olympusmicro.com/primer/techniques/oblique/obliqueintro.html> (accessed  
 September 19, 2012)
56. Nikon ME 600 DIC, information page,  
<http://www.nanophys.kth.se/nanophys/facilities/nfl/nikon-me600/dic.html> (accessed August 25,  
 2012).

57. Polarizing, 2012. Nikoninstrument.com. <http://www.nikoninstruments.com/Information-Center/Polarizing2> (accessed August 26, 2012)
58. Introduction to optical birefringence, 2010-2012. Microscopyu.com. <http://www.microscopyu.com/articles/polarized/birefringenceintro.html> (accessed August 26, 2012).
59. Dorset, L. D. *Macromolecules*, **1986**, *19*, 2965.
60. Ikeda, S.; Kiguchi, M.; Yoshida, Y.; Yase, K.; Mitsunaga, T.; Inaba, K.; Saiki, K. *J. Cryst. Growth* **2004**, *265*, 296.
61. Baker, T. R.; Mougous, D. J.; Brackley, A.; Patrick, L. D. *Langmuir* **1999**, *15*, 4884.
62. Shimizu, H.; Tanigaki, N.; Nakayama, K. *J. Appl. Phys.* **1994**, *34*, 701.